hydrogen

MDPI

Review

The Effect of Electrolytes on the Kinetics of the Hydrogen Evolution Reaction

Goitom K. Gebremariam [1,2], Aleksandar Z. Jovanović [1] and Igor A. Pašti [1,*]

[1] Faculty of Physical Chemistry, University of Belgrade, Studentski trg 12–16, 11158 Belgrade, Serbia; nebyat1997@gmail.com (G.K.G.); a.jovanovic@ffh.bg.ac.rs (A.Z.J.)
[2] Department of Chemistry, Mai Nefhi College of Science, National Higher Education and Research Institute, Asmara 12676, Eritrea
* Correspondence: igor@ffh.bg.ac.rs; Tel.: +381-11-3336-625

Abstract: Amid global energy challenges, the hydrogen evolution reaction (HER) is gaining traction for green hydrogen production. While catalyst research is ongoing, recognizing electrolyte effects remains crucial for sustainable hydrogen production via renewable-powered water electrolysis. This review delves into the intricate effects of electrolytes on the kinetics of the HER. It examines key factors including the pH, cations, anions, impurities, and electrolyte concentration. This review discusses the notion that the electrolyte pH alters catalyst–electrolyte interactions and proton concentrations, thereby influencing factors such as the hydrogen binding energy, water adsorption, and overall reaction kinetics. Moreover, this review provides a briefing on the notion that electrolyte cations such as Li^+ can impact the HER positively or negatively, offering opportunities for improvement based on the metal substrate. Interestingly, there is a potential that the HER can be tuned using Li^+ ions to modify the M–H bond energy, demonstrating a flexibility beyond the pH levels and counter-ions. The varied adsorption energies of metal cations on metal electrodes are also found to influence the HER kinetics. The effects of electrolyte anions and impurities are also discussed, emphasizing both the positive and negative impacts on HER kinetics. Moreover, it is pointed out that the electrolyte-engineering approach enhances the HER kinetics without permanent catalyst surface modifications. This review underscores the importance of the electrolyte composition, highlighting both the challenges and potential solutions in advancing HER research for sustainable energy production.

Keywords: hydrogen evolution reaction; kinetics; electrolyte; electrolyte ions; electrolyte impurities; electrolyte engineering

Citation: Gebremariam, G.K.; Jovanović, A.Z.; Pašti, I.A. The Effect of Electrolytes on the Kinetics of the Hydrogen Evolution Reaction. *Hydrogen* **2023**, *4*, 776–806. https://doi.org/10.3390/hydrogen4040049

Received: 13 September 2023
Revised: 7 October 2023
Accepted: 9 October 2023
Published: 13 October 2023

1. Introduction

1.1. Background Information on the Hydrogen Evolution Reaction

In the 21st century, pressing issues include the depletion of non-renewable energy sources, the environmental harm from fossil fuels, and the escalating global energy demand. With fossil fuels being responsible for 84% of energy consumption, their use leads to severe environmental issues. Researchers are investigating renewable energy sources such as solar, wind, and biomass sources to address the environmental problems and growing energy demands. However, these sources are intermittent, necessitating the use of efficient energy transformation and storage technologies. Efficient energy storage methods are vital for a reliable energy supply, especially with the rise of renewables, with an emphasis on electrochemical energy storage systems like batteries. However, these systems lead to environmental issues due to their material toxicity and energy-intensive manufacturing processes. Thus, hydrogen, renowned for its high energy density and emission-free combustion by-product, is a widely explored energy carrier, while water splitting utilizing surplus electricity from renewables holds promise for clean hydrogen production [1]. This method ensures a high energy conversion efficiency [2–4], promoting its use in fuel cells

or combustion for a greener future [5–8]. As summarized in [9], global hydrogen demand is expected to surpass 500 Mt by 2050, generating around USD 3 trillion in revenue [10]. Currently, 95% of hydrogen comes from so-called grey hydrogen, emitting 10 kg of CO_2 per 1 kg of hydrogen produced. Green hydrogen from water electrolysis by renewable sources is eco-friendly but costs about four to five times more than grey hydrogen due to electricity expenses [11]. Thus, improving the efficiency of water electrolysis technologies is crucial to achieving lower production costs.

Solar water splitting is anticipated to serve as the cornerstone of a sustainable hydrogen-based energy economy. This process offers a carbon-neutral means of producing hydrogen gas, utilizing abundant renewable resources—water and sunlight. Ref. [12] provides a comprehensive review of the current state of direct water splitting in photo-electrochemical cells (PECs). The study includes a case study using a simple solar cell with efficient water-splitting electrodes and a detailed mechanism analysis. Additionally, the review offers an in-depth analysis of the energy balance and efficiency in solar hydrogen production. A demonstration employing a ~0.7%-efficient n-Si/Ni Schottky solar cell connected to a water electrolysis cell was observed to attain an impressive 52% solar hydrogen production efficiency. Emphasizing the separation of solar harvesting and electrolysis processes prevents photo-electrode corrosion and optimizes electrodes for the HER and OER; this approach attains ~10% efficiency when paired with conventional 18%-efficient Si-solar cells commonly used on household roofs. The review also outlined a strategy to surpass 15% efficiency for a single junction cell.

Water electrolysis involves two simultaneous electrochemical reactions, the hydrogen evolution reaction (HER) at the cathode and the oxygen evolution reaction (OER) at the anode, occurring in a typical cell with an anode, cathode, power source, and electrolyte [2,13]. The theoretical minimum energy for water splitting is 1.23 V at ambient temperature [13]. However, due to the polarization overpotential of the cathode and anode and the internal resistance of the electrolyte, additional energy is required, known as the cell overpotential [14,15]. Efficient electrocatalysts are crucial for both the HER and OER processes to improve the energy conversion efficiency and minimize overpotential. In spite of the fact that the HER is vital for transforming electrical energy into chemical energy in the form of an H_2 molecule, the OER also plays a significant part in the overall efficiency of an electrolyzer unit because of its intricate reaction mechanism [1].

This review focuses on how electrolyte affects the HER in electrochemical water splitting. Despite this emphasis, it is noteworthy that the OER imposes more significant constraints on the overall process. The lower overpotentials observed for the HER, compared to the OER, are primarily attributed to the comparatively sluggish kinetics of the OER. Thermodynamically, a voltage as low as 1.23 V is theoretically ample for the electrolytic splitting of water into O_2 and H_2, because $E^o_{O2/2H2O}$ = 1.23 V and $E^o_{2H+/H2}$ = 0 V in standard conditions. Nevertheless, it is evident that, at ΔE = 1.23 V, the current density is observed to be zero [12]. Modern alkaline electrolyzers typically function at voltages above 1.8 V, with considerable rates of the HER and the OER occurring between 2.0 to 2.5 V.

As elaborated in [12], the OER mechanism on an oxidized metal electrode surface should involve the formation of hydrogen peroxide (H_2O_2) as an intermediate. This is followed by the oxidation of H_2O_2 to O_2, involving a cascading water oxidation process from the oxidation state of oxygen (−2) in water to (−1) in peroxide, ultimately reaching 0 in a free gas:

$$2H_2O - 2e^- \rightleftharpoons H_2O_2 + 2H^+ \qquad E^o = 1.77\ V \tag{1}$$

$$H_2O_2 - 2e^- \rightleftharpoons O_2 + 2H^+ \qquad E^o = 0.68\ V \tag{2}$$

The arrangement of the E^o values for Reactions (1) and (2) indicates that, once H_2O_2 is generated, it undergoes spontaneous oxidation to produce O_2. However, this process is

notably slow at lower electrochemical potential values. The formal equation for the OER is derived by dividing the sum of these two reactions by 2:

$$H_2O - 2e^- \rightleftharpoons 1/2O_2 + 2H^+ \qquad E^o = 1.23\ V \tag{3}$$

while the process, actually, does not follow this path. Therefore, Reaction (1) with $E^o = 1.77$ V should be considered to be the main energetic barrier in the H_2O-splitting process.

The study utilized a water photoelectrolysis cell with a Pt cathode and a Ti/(Ir-Ta) oxide anode connected to an n-Si/Ni Schottky solar cell battery. When the illumination on the solar cell was turned OFF, the cell voltage stabilized at 0.68 V, supporting the suggested water-splitting mechanism involving an H_2O_2 intermediate. Upon turning OFF the illumination, electrolysis halts, and the Pt cathode potential remains temporarily at 0 V. Simultaneously, the anode maintains the potential of the redox couple O_2/H_2O_2 as per Equation (2).

Water oxidation, thermodynamically feasible at 1.23 V, can be depolarized between 1.23 V and 1.77 V with the appropriate electrocatalysts. The mechanism of the electrocatalytic OER taking place on the Ni electrodes and involving the formation of metal surface peroxide species has been proposed [16]. Based on experimental findings and existing literature, it is proposed that, in alkaline conditions at $E \approx 1.5$ V (RHE), there is a reversible electrochemical generation of Ni(IV) peroxide described by the reaction: $NiO(OH)_2 + 2OH^- \rightleftharpoons NiOO_2 + 2H_2O + 2e^-$. This reaction explains the underpotential O_2 formation from $NiOO_2$ peroxide (with respect to $E^o{}_{H2O2/H2O} = 1.77$V), as well as the observed low dE/dlog(i) slope (<60 mV) at low anodic current densities, indicative of a two-electron transfer process.

During photolytic water splitting on a semiconductor surface, a 1.23 eV photon breaks one O–H bond in an H_2O molecule. To break both bonds, two such photons (equivalent to ~2.46 eV) are needed, similar to the energy released when one mole of H_2 gas is burned in O_2. This work can also be accomplished by two photons with energies ≥ 1.77 eV + 0.68 eV or a single photon with energy ≥ 2.46 eV. In terms of energy, electrolytic and photolytic water splitting incur similar costs. The low probability of the direct reaction in Equation (3) could be attributed to nonlinearity, where two water molecules exchanging four electrons contrasts with Equation (1), where only two electrons are involved, making the latter pathway more probable due to the space-time synchronization in the electrochemical reaction [12].

Amid the global energy crisis, there is a rising interest in the HER to produce pure (green) hydrogen using renewable energy sources. Researchers are actively exploring new and cost-effective catalysts for HER to make this process economically viable. The HER volcano curves [17–19], based on Sabatier's principle, are valuable tools in understanding trends in HER activity, aiding in the search for optimal electrocatalysts by analyzing the reaction rate against the free energy of adsorption for intermediates [2].

Depending on the type of electrolyte employed, water electrolysis can take place in acidic, pH-neutral, or alkaline conditions. Equations (4) and (5) outline the corresponding HER reactions in acidic and alkaline electrolytes, respectively:

$$2H^+ + 2e^- \rightarrow H_2 \tag{4}$$

$$2H_2O + 2e^- \rightarrow H_2 + 2OH^- \tag{5}$$

The mechanism of the HER, which is influenced by the pH of the solution [20], can be summarized in acidic environments as follows (* is an empty adsorption site):

$$H^+ + e^- + * \rightarrow H_{ads} \tag{6}$$

$$H_{ads} + H_{ads} \rightarrow H_2 + 2* \tag{7}$$

$$H^+ + H_{ads} + e^- \rightarrow H_2 + * \quad (8)$$

In an alkaline media, the HER mechanism can be presented in a similar way:

$$H_2O + e^- + * \rightarrow H_{ads} + OH^- \quad (9)$$

$$H_{ads} + H_{ads} \rightarrow H_2 + 2* \quad (10)$$

$$H_2O + H_{ads} + e^- \rightarrow H_2 + OH^- + * \quad (11)$$

Within the above-presented mechanisms, * signifies an unoccupied active site on the catalyst's surface. The reaction is initiated with a Volmer step (Equations (6) and (9)), and the intermediate species (H_{ads}) is subsequently eliminated from the surface via either the Tafel reaction (Equations (7) and (10)) or the Heyrovsky reaction (Equations (8) and (11)). The HER on Pt and PGMs is rapid and reversible at a low pH, but cost and scalability issues demand alternative catalysts. Cheaper metals like Ni hold potential as alternatives to Pt for the HER, but they exhibit lower performance and stability issues in acidic conditions. In alkaline media, the HER is notably slower, even on Pt, mainly due to the sluggish H_2O dissociation step (Equation (9)). PGMs still have excellent HER performance in alkaline environments, but their activity declines by ~2 order of magnitude compared to acidic media [21], emphasizing the impact of the electrolyte in the HER.

However, it is important to note that studies by [22,23] have challenged the classical HER mechanism. In particular, [22] reexamined the mechanisms of a reversible HER and HOR through thermodynamic analysis and a recent literature review. Contrary to the long-standing assumption involving H_{ad} atoms as intermediates, the study proposed that the adsorbed molecular ion $(H_2^+)_{ad}$ serves as the intermediate in both HER and HOR reactions, aligning better with contemporary experimental observations. Moreover, [24] analyzed experimentally reported data with models which provide a quantitative match [25]. The analysis suggests that the reversible electrochemical hydrogen evolution (H_2ER) occurring in acidic, neutral, and alkaline aqueous solutions can be described by one common reaction (Equation (14)), which involves an intermediate stage of the adsorbed hydrogen molecular ion (H_2^+) instead of H_{ad} as postulated in the typical Volmer–Heyrovsky–Tafel mechanism. The distinctive characteristics of this reaction are as follows: (i) it entails the transfer of two electrons for each H_3O^+ and OH^- ion; (ii) the precursor of the H_2 molecule is the molecular hydrogen ion $(H_2^+)_{ad}$, which forms during the transfer of the first electron (Equation (12)), with the second electron transfer leading to the formation of H_2 (Equation (13)); (iii) the energy of hydration preserved within the H_3O^+ ion is utilized for the bond formation in the H_2 molecule and accounts for the depolarization of the H^+ discharge from $E^o_{H+/H} = -2.106$ V (SHE) to $E > 0$ V, known as the H_{UPD} phenomenon observed on Pt. Considering these factors, the formation of H_{ad} as an intermediate in the HER/HOR appears to be both thermodynamically and kinetically unfavorable.

In the reversible region of the hydrogen evolution, theoretical analysis indicates two possible slopes of potential vs. log(i) plots: 2.3 RT/F ≈ 60 mV and 2.3 RT/2 F ≈ 30 mV. This aligns with findings in the literature on the electrocatalytic hydrogen evolution, serving as evidence for the alternative mechanism described herein. Recent experimental results on Pt electrodeposition [25] align with the presented analysis, providing support for the mechanism, involving the formation of H_2^+ as an intermediate in the reversible hydrogen evolution on Pt. As the transition to the irreversible hydrogen evolution occurs, a slowdown in the formation of H_2^+ in the first electron transfer stage manifests, leading to an increased slope of 2.3 RT/0.5 F ≈ 120 mV (here, R, F, and T represent the universal gas constant, Faraday constant, and absolute temperature, respectively). The processes occurring at $E = 0$ V (SHE) can be described by the following sequence of electrochemical reactions:

$$H_3O^+ + e^- \rightleftharpoons (H_2^+)_{ad} + OH^- \quad (12)$$

$$(H_2{}^+)ad + e^- \rightleftharpoons H_2 \quad (13)$$

The overall reaction is:

$$H_3O^+ + 2e^- \overset{(H_2{}^+)_{ad}}{\rightleftharpoons} H_2 + OH \quad (14)$$

Near the equilibrium potential, both processes (12) and (13) occur rapidly and reversibly and proceed simultaneously, leading to an overall two-electron process (14). This process characterizes redox reactions on a Pt surface within specific rate limits in an RHE. It plays a key role in determining the exchange current (i_0) magnitude and the potential (E) of the overall electrochemical process.

Numerous water electrolysis techniques have been studied and can be categorized according to the electrolytes used. These methods encompass proton exchange membrane electrolysis (PEMEL) and alkaline electrolysis, which includes both traditional alkaline water electrolysis (AEL) and anion exchange membrane electrolysis (AEMEL) [2,7,13,26]. Although both AEL and PEMEL have attained high degrees of technological maturity [26], it is still challenging to produce hydrogen on a large scale using water electrolysis due to the high cost of PGM catalysts in acidic conditions and the low energy conversion efficiency of non-PGM catalysts in alkaline conditions. Moreover, the local acidic environment in PEMELs severely restricts the selection of electrocatalysts to a small subset of PGMs [27]. On the other hand, alkaline water splitting, employing a cost-effective KOH electrolyte, enables the use of affordable non-PGMs such as Ni, offering advantages over PEMEL cells. In practical applications, large-scale water electrolysis is carried out in concentrated alkalis, utilizing stable and inexpensive Ni-based catalysts, whose decreased activity relative to Pt is offset by their lower price [20].

The kinetics of the HER can be influenced by different factors, including the nature and composition of the electrolyte, the crystal shape and orientation of the electrode (single-crystal, polycrystalline, amorphous, etc.), and many other factors. This review will discuss the effect of the nature and concentration of the electrolytes on the kinetics of the HER.

1.2. Importance of Studying the Kinetics of the HER

Based on the elementary processes (Equations (3)–(5)), it is conceivable to imagine two potential mechanisms in acidic conditions, Volmer–Tafel and Volmer–Heyrovsky [28], and the preferred mechanism depends on various factors, including the surface coverage of H_{ads} and the overpotential applied. In situations where the surface coverage is high, there is a higher likelihood of the Volmer–Tafel mechanism occurring due to the increased probability of the surface recombination step. Conversely, when the surface coverage is low, the Volmer–Heyrovsky mechanism is favored [2]. The Volmer–Tafel pathway is more common at low overpotentials, while the Volmer–Heyrovsky becomes more prevalent as the overpotential increases [29]. The above-mentioned mechanisms can result in three possible rate-determining steps (RDSs): Volmer, Heyrovsky, and Tafel. Both mechanisms exhibit an exponential increase in the catalytic current with overpotential. Still, the rate of increase differs for different RDSs, allowing for the identification of the RDS and the surface mechanism of a catalyst [28]. Previous studies [30–34] have suggested that the Volmer step is the RDS for the kinetics of the HER/HOR on polycrystalline Pt surfaces. Conversely, some other studies [35,36] suggest that the Heyrovsky step controls the kinetics of the HER.

The Tafel slope provides information about the RDS and the plausible HER mechanism, specifically related to the electron-transfer kinetics in the catalytic reaction. A smaller Tafel slope indicates faster electrocatalytic kinetics, leading to a higher current density (j) with a lower overpotential. The exchange current density (j_0) refers to the charge transfer rate under equilibrium conditions. A greater j_0 signifies an accelerated charge transfer rate and a diminished reaction barrier [28]. Thus, a better electrocatalyst typically has a lower Tafel slope and a higher j_0 [37]. In the HER potential region at 25 °C, different Tafel slopes are theoretically predicted based on the RDS, i.e., -120 mV dec^{-1}, -30 mV dec^{-1},

and -40 mV dec^{-1} for the Volmer, Tafel, and Heyrovsky limiting reactions, respectively. Typically, a Tafel slope of -120 mV dec^{-1} is observed on most materials at practical current densities. This finding is attributed to the slow discharge of protons or the sluggish electrochemical desorption of H_{ads} atoms. However, in acidic environments where the Volmer step is exceptionally rapid, PGMs tend to exhibit a lower Tafel slope of -30 mV dec^{-1}. While the literature commonly associates a Tafel slope of -120 mV dec^{-1} with the Volmer step for the HER, Shinagawa et al. showed that this slope can also be obtained when the Heyrovsky step is the RDS at high H_{ads} coverage (>0.6) [36].

Moreover, there is a scenario where different steps proceed at a similar rate, making the Tafel slope analysis uncertain [21]. Watzele et al. discussed the challenges and uncertainties in understanding the HER. The authors used electrochemical impedance spectroscopy to study the relative contributions of two pathways (Volmer–Heyrovsky and Volmer–Tafel) to the HER at different electrode potentials and pH values. Their results showed that both pathways contribute similarly to the reaction, and neither dominates [38]. Electrocatalytic kinetics, unlike outer-sphere reactions, are intricate due to adsorbed intermediates. The Butler–Volmer equation must account for the variable surface coverage of these species influenced by the electrode potential, posing challenges in the Tafel slope interpretation, notably in the HER and similar processes. Thus, not only is the HER mechanism identification based on the Tafel slope difficult, it can also be very misleading.

1.3. Definition and Types of Electrolytes Used in HER Studies

Various electrolytes are used for HER studies. They can differ by pH (acidic, neutral, or alkaline) or solvent (such as organic solvents or ionic liquids). The choice of electrolytes significantly impacts the efficiency of the HER [15]. The majority of the research on the HER mechanisms and the activity of different materials has been conducted under kinetically preferred, extremely acidic [17,39–42], and alkaline aqueous conditions [42–47] while there has also been significant attention on studying the HER under near-neutral pH conditions [48–52]. Acidic electrolytes used for the HER include H_2SO_4 [17,18,53,54], HCl [55,56], and $HClO_4$ [42,55,57,58]; and the most commonly used alkaline electrolytes include NaOH [59,60] and KOH [19,42,45,55,57,61–67]. At the same time, the use of LiOH can also be found in the literature [55]. Besides the traditional liquid electrolytes, other types of electrolytes, such as solid electrolytes and ionic liquids (ILs), are also investigated for the HER. ILs are utilized in electrochemical systems for an efficient HER due to their exceptional properties, such as low vapor pressure, high electrical conductivity, and a wide variety of functional groups [15]. For example, Amaral et al. [68] studied the impact of adding an ionic liquid (IL) ([Emim][$MeSO_3$]) to a Pt cathode in an 8 M KOH solution at temperatures from 25 to 85 °C. The IL addition exhibited a catalytic effect, increasing j_0 and reducing overall impedance up to 45 °C. The activation energy for the HER in the IL-added KOH was 10 kJ mol^{-1} compared to the IL-free KOH solution.

1.4. Significance of Electrolytes in HER Kinetics

In general, the HER is performed in highly acidic or highly alkaline electrolytes, and the nature of the electrolyte plays a significant role in the kinetic of the HER. Due to the availability of higher concentrations of H_3O^+ ions, the HER on PGMs in acidic solutions is remarkably fast. However, its efficiency is limited by the diffusion of hydrogen ions from the bulk of the solution to the electrode–electrolyte interface where the concentration is not sufficiently high [42]. Furthermore, the acidic environment significantly limits the catalyst options to only a few scarce and costly PGMs [27]. Conversely, the HER in alkaline electrolytes is relatively slow, but it allows us to use affordable non-PGMs. Besides strongly acidic/alkaline electrolytes, the HER can also occur in neutral and near-neutral electrolytes. These electrolytes provide benefits like reduced corrosion and a wider range of electrocatalysts without the need for specialized membranes or acid/alkali-resistant catalysts [69,70]. Furthermore, neutral environments facilitate the utilization of seawater as an electrolyte and the desegregation of metal-based electrocatalysts with biocatalysts

to produce biofuels [2]. Merrill et al. [71] found that protonated weak acids in microbial electrolysis cell (MEC) solutions affect the HER through weak acid catalysis and reducing solution resistance. The study emphasized the importance of specific buffers in optimizing the MEC efficiency across different pH ranges, with phosphate and acetate working better in acidic conditions and carbonate at a higher pH due to the increased conductivity.

Recent research has demonstrated that the interactions between the electrolyte and the electrocatalyst significantly influence the electrocatalytic properties. The electrolyte's impact on the electrochemical reactions occurs through two mechanisms: (i) via the chemisorption of adsorbents in the inner Helmholtz layer involving the electron transfer, and (ii) through weak van der Waals interactions between the electrode and spectator (supporting) ions in the electrolyte at the outer Helmholtz layer [72,73]. The kinetics of the HER in an aqueous medium are typically influenced by two adsorbates: H_{ad} in acidic conditions and OH_{ad} in alkaline conditions. For example, Strmcnik et al. found that OH_{ad} plays a crucial role in the HER over H_{ad} for Pt in an alkaline medium [50]. However, conflicting reports have led to ongoing debates in this regard [74].

For a long time, the hydrogen binding energy (HBE) of the metal catalyst surface or the energy of the M–H bond ($\Delta E_{M\text{-}H}$) were outlined as a factor influencing the HER rate, starting with the classical works of Trassati studying the HER in acidic media. Sheng et al. experimentally demonstrated that the hydrogen desorption peaks of underpotential deposited hydrogen (H_{UPD}) on Pt(100) and Pt(110) are directly linked to the metal HBE and are pH-dependent [75]. Increasing pH levels led to an increased HBE on Pt, resulting in a decrease in Pt's HER activity. Koper et al. demonstrated that spectator ions such as alkali metal cations, viz., Li^+, Na^+, K^+, and Cs^+, have the ability to weaken the metal–OH_{ad} bond (M-OH_{ad}), resulting in an elevation of the interfacial pH and a subsequent positive shift in the H_{UPD} desorption peak [76]. Later on, it was found that not only the pH values of the electrolyte but also the co-adsorption of alkali metals such as K are responsible for the positive shift in the H_{UPD} desorption peak of Pt by weakening the Pt-OH_{ad} bond. Recent research indicates that aqueous electrolytes containing alkali metal cations, specifically Li^+, can effectively enhance various electrochemical reactions, including those in batteries, carbon dioxide reduction, and nitrogen reduction [73].

The use of Li^+-containing aqueous electrolytes is not yet commercialized, making HER suppression necessary in certain processes [77]. Suo et al. discovered that highly concentrated lithium bis(trifluoromethanesulfonyl)imide (LiTFSI)-based aqueous electrolytes (>5 M) can achieve a water-in-salt condition and enhance the water stability window to ~2.9 V [78]. However, at higher LiTFSI concentrations, $TFSI^-$ ions can split to form F^-, which creates an LiF layer on the active electrode (stainless steel), selectively blocking the diffusion of H^+ ions. Guha et al. discovered that the observed phenomenon in the presence of Li^+ goes beyond the formation of LiF and is independent of the supporting anion ($TFSI^-$), particularly when working with high Li^+ concentrations rather than low concentrations as in previous reports [79]. They found that Pt electrodes suppress the HER at all pH values, while, for bulk gold (Au), HER activities are enhanced with Li^+. The study suggested that the M/Li^+ interaction plays a significant role in this phenomenon, and the enhanced H_2(g) production with Au was confirmed using gas-chromatography-based quantifications.

2. Influence of Electrolyte Composition on HER Kinetics

2.1. Effect of Electrolyte pH on HER Kinetics

The influence of the electrolyte pH on the rate of the HER was overlooked due to the experimental limitations in assessing rapid kinetics in acidic media. Nevertheless, it is now evident that pH strongly affects the HER, particularly on highly active metals. For instance, when moving from pH = 0 to pH = 13, the HER activities of Pt, Ir, and Pd drop by factors of 210, 120, and 90, respectively [43,80]. On the other hand, non-PGM electrodes, such as Au, Ni, or Cu, experience a lesser impact, with a 10-fold reduction in HER activity [17,19,80]. Additional studies conducted in neutral solutions have shown that the decrease in activity directly correlates with the pH level [75]. Experimental findings show that the HER activity

of various electrocatalysts progressively declines with the rise in pH [50]. A significant decrease in HER activity for Pt(111), Au(111), and polycrystalline Ir (Ir_{pc}) was observed with increasing pH (pH = 1 to 13) [81]. Au(111) displayed higher overpotentials than Pt(111) and Ir_{pc} at the same current density in acidic pH, attributed to the mass transport of reactive H_3O^+ species regulating the HER [49]. However, above pH = 5 and certain potentials, metal polarization curves became pH-independent, suggesting the H_2O to H_2 transformation dominated the HER currents. Thus, the main difference between the HER in alkaline and acidic media is that the HER in alkaline solutions is limited by a sluggish water dissociation step (Equation (6)) [50].

Examining the impact of surface-dependent kinetic rates is another way to investigate how the pH of the electrolyte affects the HER. In particular, while the activity of Pt low-index single-crystal surfaces varies only slightly in acidic media, it varies significantly in alkaline solutions [39,44,82]. According to Danilović et al. [83], the highly defected Pt(110) exhibits higher activity compared to the relatively "perfect" Pt(111). Moreover, the variation in activity is explained by the fact that the adsorption of the hydroxyl and H_{UPD} species is influenced by the structure of the crystal surface, which ultimately impacts the formation of the electroactive intermediate, H_{OPD} [45]. For a more thorough understanding of the HER's structure–activity relationship, Marković et al. [81] have conducted a comparative study between the HER activity of Pt(111) and Pt(111) decorated by electrochemically deposited Pt islands (Pt-islands/Pt(111)). In alkaline media, the Pt-islands/Pt(111) surface exhibited a five- to six-times-higher HER activity compared to the pristine Pt(111), while in acidic media, the enhancement was only around 1.5 times. The pH effect shows that low-co-ordinated single-crystal Pt atoms play a crucial role in increasing the rate of the HER in alkaline solutions, promoting the dissociative adsorption of water [81].

In the current literature, several prevailing hypotheses explain why HER kinetics are slower in alkaline solutions than in acidic ones:

(i) The HBE is pH-dependent [19,75,84]. This concept has helped to explain numerous experimental findings, even though some inconsistencies still exist [81,84,85]. For illustration, if the HBE were to increase, it would account for the positive potential shift of the H_{UPD} on the PGM electrodes when they change from an acidic to an alkaline electrolyte. Nevertheless, despite demonstrating considerably lower HER activity in alkaline electrolytes than in acidic ones, the Pt(111) surface remains largely unaffected by this shift caused by the H_{UPD} [80,86,87]. Furthermore, if there were a universal increase in the HBE with pH, it would enhance the HER electrocatalytic activity of metals that weakly bind hydrogen (such as Au). However, this contradicts the experimental observations [80].

(ii) The proton donor (H_3O^+ or H_2O) is pH-dependent [50]. In other words, the proton donor can switch from H_3O^+ in an acidic environment to H_2O in an alkaline environment.

(iii) At the electrode | electrolyte interface, there is a pH-dependent water reorganization energy. According to Koper et al. [88], the water-reorganization energy related to the proton–electron transfer would be higher because interfacial fields are stronger in an alkaline environment. Rossmeisl et al. [89] initiated an attempt to address the pH in the density functional theory (DFT) calculation and, applying the scheme to the Pt(111) | electrolyte(water) interface as an example, they have observed that the adsorbate coverage and water orientation were affected by the pH [89]. Recent studies by Rossmeisl et al. have associated the reduction in HER activity at a high pH with changes in the configurational entropy of the proton as it crosses the outer Helmholtz plane [90]. Cheng et al. [91] carried out full solvent quantum mechanics molecular dynamics (QMMD) simulations to explicitly simulate the water/Pt(100) interface at an applied voltage (U) from +0.29 V to −0.46 V, which is equivalent to a pH from 0.2 to 12.8 at U = 0.3 V (RHE). The study deduced that the pH-dependent HBE on the noble metal is mostly caused by changes in water adsorption. They discovered that

the electrode exhibited a tendency to repel water as the applied voltage was made more negative, which, in turn, boosted the hydrogen binding.

The HER mechanism in neutral solutions is proposed to be similar to that of the alkaline media, proceeding through the adsorption step (Equation (6)), followed by the desorption steps (Equations (7) or (8)). In near-neutral pH with typical supporting electrolytes like Na_2SO_4 or $NaClO_4$, the HER relies on water as the primary reactant for significant hydrogen production. Due to the reduced hydronium ion activity in these circumstances, reactant mass-transport flux becomes slower than the surface hydronium ion reduction rate. As a result, in unbuffered near-neutral-pH electrolyte solutions, a significant amount of overpotential is needed to achieve greater current densities than in acidic or alkaline pH conditions [92]. In pH-neutral electrolytes, the HER process involves a two-step reduction process. In contrast, in strongly acidic or alkaline electrolytes, the reduction occurs in a single step with H_3O^+ ions or H_2O molecules, respectively [93]. During the initial reduction phase of the HER, the main reactants are H_3O^+ ions, and this occurs at low cathodic overpotentials. As the overpotential increases, the HER process becomes diffusion-controlled, where a constant current is observed [52]. The second reduction phase takes place at higher overpotentials, during which the principal reactants in the HER change from H_3O^+ ions to H_2O molecules, leading to a steady rise in the reduction current [69]. For instance, the HER electrocatalytic performance of Pt in the pH range of 5 to 9 does not align with the predicted shift in the thermodynamic potential (i.e., −59 mV per pH unit) [51]. The Mayrhofer group [48] discovered that, in unbuffered or inadequately buffered electrolytes, the pH near electrode surfaces significantly deviates from the bulk electrolyte pH, particularly in the range of pH 4 to 10 (Figure 1). These observations suggest that the kinetics of the HER in pH-neutral conditions behave uniquely.

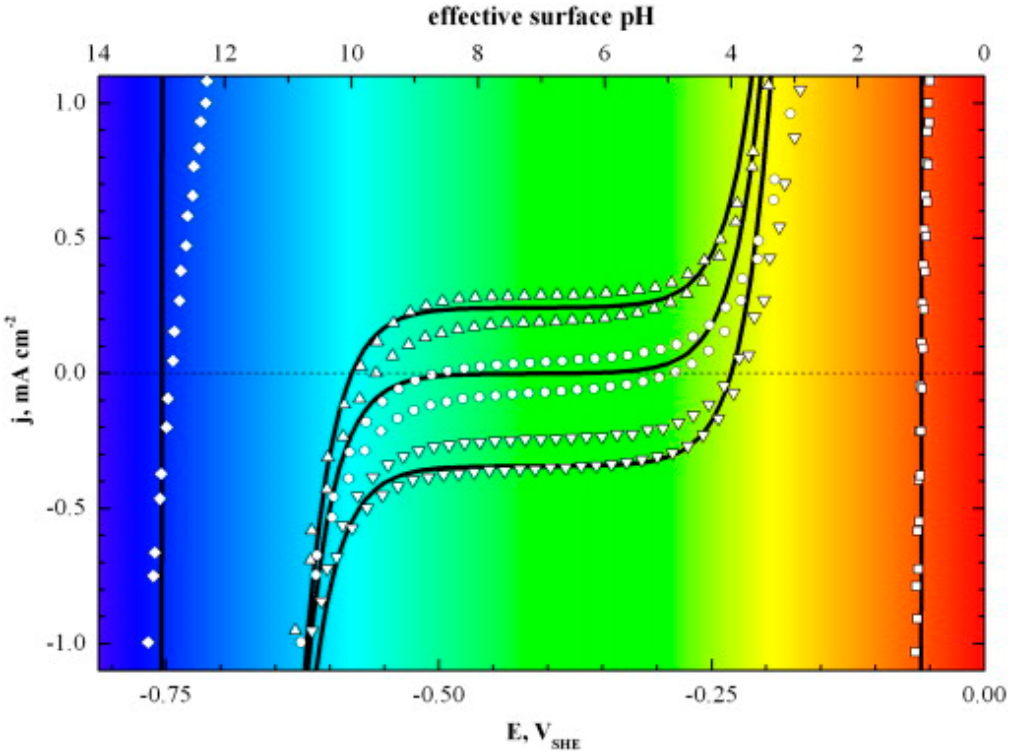

Figure 1. Current density–surface pH relation obtained by cyclic voltammetry (rotation rate: 1600 rpm; scan rate: 10 mV s^{-1}) in H_2-saturated, unbuffered solutions of bulk pH values equal to (□) 1, (▽) 4, (○) 7, (Δ) 10, and (◊) 13. The solid lines denote the predictions for the corresponding solutions as derived from Equation (5). The effective surface pH is indicated at the top and by the underlying color scheme. Reproduced from/Reprinted from Ref. [48] with permission from Elsevier.

Furthermore, Takanabe's research team uncovered that the HER processes in near-pH-neutral solutions are influenced by the nature of the reactants, the state of the electrolytes (buffered or unbuffered), and their concentrations [51,52,94]. They investigated the relationship between the HER and the pH using various unbuffered 0.5 M Na_2SO_4 solutions. They found that the HER activity is based on the activity of H_3O^+ ions rather than the nature of the supporting electrolyte (Figure 2). Depending on the theoretical diffusion-limited current density, the authors categorized the HER activity into three pH regions: acidic (1–5), neutral (5–9), and alkaline (9–13) [51]. The neutral region was found to have insufficient H_3O^+ ions, limiting the HER activity.

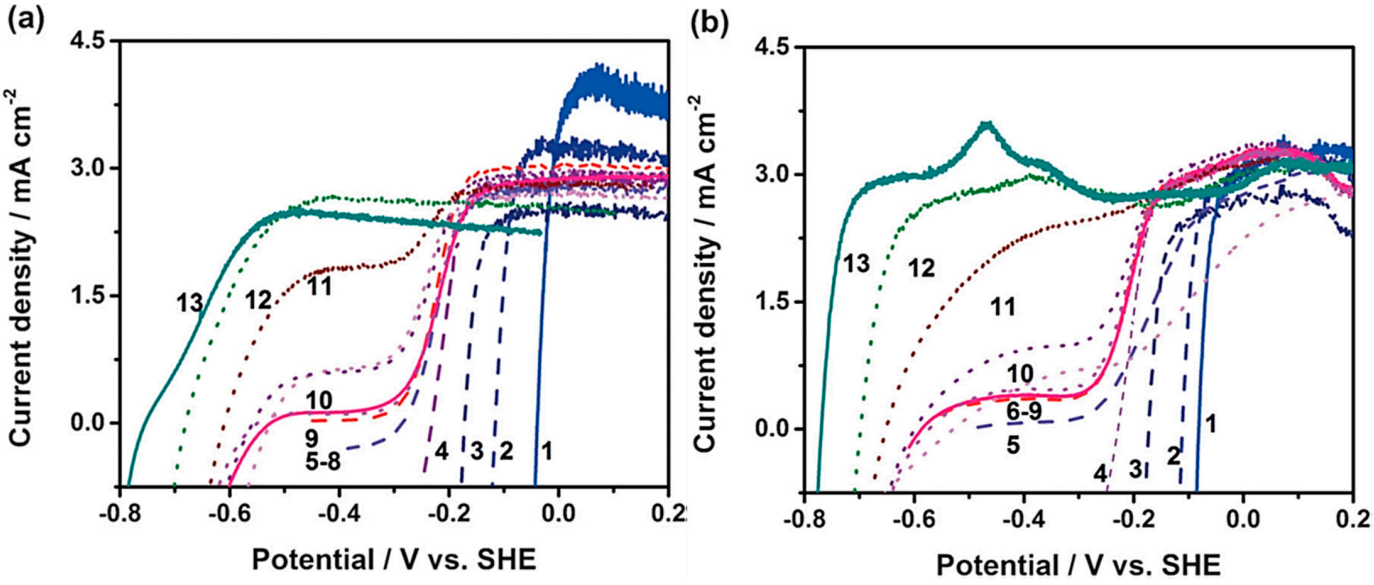

Figure 2. Linear sweep voltammograms for HOR using (**a**) Pt disk and (**b**) Pt/C electrodes at a rotation rate of 3600 rpm in the positive direction. Conditions: H_2, Na_2SO_4 (0.5 m), 298 K, and 50 mV s^{-1}. Reprinted from Ref. [51] with permission from Wiley.

Yet, the supply of H_3O^+ ions can be enhanced by buffered electrolytes, which helps overcome the limited H_3O^+ ion availability near electrode surfaces [52,92,95]. Research has been focused on improved an neutral-pH performance using buffered solutions [48,49] such as phosphate, borate, and carbonate [71,96–98], yielding onset potentials similar to acidic and alkaline conditions [49,71]. Koper et al. [99] have investigated the HER in bicarbonate-containing electrolytes on Au and Pt electrodes and observed an enhanced HER rate with a bicarbonate buffer despite maintaining a constant bulk pH. Additionally, there was a notable alteration in the reaction mechanism, with the Tafel Slope in bicarbonate mirroring that in acidic conditions (100 mV dec^{-1} on Au and 40 mV dec^{-1} on Pt). The observed result stems from the controlled pH near electrode surfaces due to ongoing reactions and buffering effects. On the other hand, some studies contend that the weak acid itself, e.g., phosphate species ($H_2PO_4^-$ and HPO_4^{2-}), is likely the reactant in buffered conditions [71,94,100]. While it remains uncertain if weak acid ions directly interact on the surface, the HER current on a Pt catalyst is primarily determined by the mass transport of a proton source (like phosphate ions) to the vicinity of the catalyst surface [92,94]. The HER activities in pH-neutral and alkaline conditions are significantly different, even though they are both thought to be influenced by the water dissociation as the RDS. Some studies suggest that the HER activity is better in neutral electrolytes, while others claim the opposite.

Yan and colleagues proposed that HBE can serve as the sole factor to account for the gradual reduction in the HER activity observed across PGM catalysts in different buffer electrolytes with a pH ranging from 0 to 13 [75,84]. According to them, HBE is higher in higher-pH electrolytes, resulting in intermediate HER kinetics in neutral electrolytes. Additionally, they recommended that OH^- can tune the HBE and affect HER activity. Shao

et al. [101] conducted a study using surface-enhanced infrared absorption spectroscopy and found that the HBE of Pt catalysts is influenced by the modified electric field, H_{ads} coverage, and Pt-H_2O, as well as H_{ads}-H_2O interactions, leading to a weakened HBE with increased pH levels; this can cause slower reaction kinetics and lower HER activity in high-pH environments. However, the HBE descriptor is insufficient to explain the HER catalytic behavior on well-defined Pt(111) surfaces [88]. According to Marković and Koper, the HER catalytic behavior on such surfaces is also determined by the presence of adsorbed hydroxyl molecules [47,50,88]. Marković et al. [81] suggested that, in alkaline environments, the HER and HOR require different types of sites for the H_{ads} and OH_{ads}, and the presence of OH_{ads} can affect the kinetics by rivalling for the same surface sites (blocking effect) or modifying the adsorption energy (energetic effect) of the active intermediates [50,81]. They proposed that the activity of the HER in alkaline solutions can be enhanced by carefully balancing the rate of H adsorption and OH desorption. Despite debates over the precise mechanisms involved, the combination of $Ni(OH)_2$ (for the strongest OH_{ads} bond strength) with Pt (for the optimal H_{ads} adsorption free energy, $\Delta_{ads}G_H$) has been found to enhance the activity of the HER in alkaline electrolytes significantly. This bi-functional tuning approach has also been favorably applied to pH-neutral solutions, suggesting that it is a viable method for speeding HER kinetics in pH-neutral solutions [69,102].

2.2. Impact of Different Cations and Anions on HER Kinetics

Researchers are working to improve catalyst activity by adjusting covalent adsorbate–surface interactions through surface electronic structure features. A current focus in electrocatalysis research is understanding the impact of spectator electrolyte species on electrode catalytic activity. In recent times, numerous instances of catalysts have been observed to exhibit catalytic activity that depends on cations [83] and the pH [57,61,84]. Recent research reveals that apparently inactive components in electrolytes have a significant impact on catalytic performance. Specifically, alkali metal cations (Li^+ to Cs^+) in high-pH aqueous electrolytes can cause notable changes in the reaction turnover frequency through noncovalent interactions with water molecules, spectator ions, surface adsorbates, and electrified interfaces [103]. Furthermore, the catalytic activity of Pt for HOR, ORR, and methanol oxidation, at 0.9 V versus RHE, is found to be cation-dependent, following the order of $Li^+ << Na^+ < K^+ < Cs^+$ [104]. Moreover, the kinetics of HER is found to be strongly affected by the nature of the cation, with Li^+ having the most significant effect [72]. These observations suggest that the chemical composition of electrolytes presents promising opportunities to tune noncovalent interactions and solvation environments at the electrified interface, potentially leading to significant changes in catalytic activity and selectivity.

Diverse studies have explored the impact of different alkali metal cations, including Li^+, Na^+, K^+, and Cs^+, on the inherent HER performance of noble metals like Pt and Au. However, these reports often present conflicting findings, while investigations on non-noble metals remain scarce [105–107]. The presence of Li^+ cations in the electrolyte was found to have a substantial impact on the HER, especially in the presence of surface oxophilic groups, surpassing the benefits of surface decoration with $M(OH)_2$ [46]. According to Subbaraman et al. [46], Li^+ has the potential to boost the inherent HER performance of Pt-$Ni(OH)_2$ composites, while the presence of Li^+ had no effect on the HER for Pt alone. The authors explained that the edges of $Ni(OH)_2$ play a key role in water dissociation, which was further amplified by the introduction of Li^+. However, the reason for (Li^+)'s ineffectiveness in the presence of Pt alone remained unclear, and the HER enhancement phenomenon was restricted to an alkaline environment. Recently, Liu et al. [108] proposed that Li^+ facilitates the elimination of adsorbed OH_{ad} from the double layer, thereby augmenting the intrinsic HER activity of the Pt-$Ni(OH)_2$ system.

Xue et al. [109] studied the role of different alkali-metal-cation-containing electrolytes in the HER activity of the Pt(pc), Pt(111), Pt(221), Ir(111), Au(111), and Ag(pc) electrodes. The study showed that the HER activity pattern of all the Pt-electrodes and that of Ir(111), regardless of their surface structure, was fairly linked to the hydration energy of the alkali

metal cations in the electrolyte, following the sequence: $Li^+ > Na^+ > K^+ > Rb^+ > Cs^+$. This pattern was reversed for the Au(111) and Ag(pc) electrodes (Figure 3). These findings prove that the presence of alkali metal cations indeed influences the HER performance of metal electrodes, with variations of ~4 times between electrolytes containing Li^+ and Cs^+. It was proposed that the observed influence may be attributed to non-covalent interactions between alkali metal cations near the catalytic centers and the adsorbed reaction intermediates at the electrode surface, or it could be due to the co-adsorption of metal cations onto the electrode surface [72,109]. The presence of cations facilitates the removal of OH_{ad} from the OH_{ad}-(H_2O)-AM^+ adduct, resulting in higher HER activity with smaller and more acidic alkali cations [110]. Weber et al. [72] also found that an enhanced activity with LiOH is linked to a lower activation energy compared to the activity observed with NaOH and KOH electrolytes.

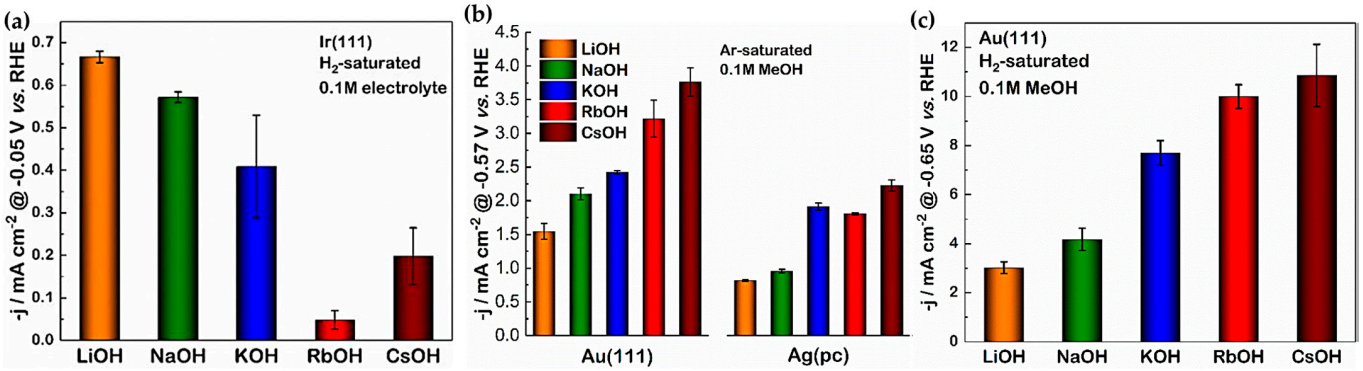

Figure 3. (**a**) The HER current densities of Ir(111) in H_2-saturated alkaline solutions at −0.05 V vs. RHE. The HER activity decreases from LiOH to CsOH, similar to that of Pt. (**b**) The HER current densities of Au(111) and Ag(pc) in Ar-saturated alkaline solutions at −0.65 V vs. RHE. The activity trend is reversed in comparison with Pt and Ir. (**c**) The HER current density of Au(111) in H2-saturated alkaline solutions at −0.65 V vs. RHE. Reprinted from Ref. [109] with permission from Wiley.

Huang et al. [111] used a classical molecular dynamics (MD) simulation to investigate the effect of structure-making/breaking cations on the kinetics of the HER/HOR of Pt(111) in the pH range from 1 to 14. They observed that the cations affected the kinetics, with j_0 increasing in the order $Cs^+ < Rb^+ < K^+ < Na^+ < Li^+$. Based on this study, electrolytes with larger (more structure-breaking) cations have more surface-bound cations than those with smaller (more structure-making) cations, leading to a cation-dependent interfacial hydrogen-bonding network. The resulting variations in interfacial water structure can influence the effective dielectric properties and fluctuations, affecting solvent reorganization energy (Figure 4). Figure 4a shows that larger cations (Cs^+) lead to the removal of water molecules from the interface due to a strong ion–surface interaction. Conversely, a stable interfacial water layer is formed with smaller cations (Li^+) (Figure 4b). By applying the Born model of reorganization energy and reaction entropy, the interfacial static dielectric constant was estimated to be notably lower than in bulk electrolyte, with the order of increase being $Li^+ < Na^+ < K^+ < Rb^+ < Cs^+$ on the negatively charged Pt RDE. This study suggests that, as cations with a stronger structure-breaking tendency (e.g., Cs^+) concentrate and partially desolvate at the electrified interface, this leads to higher static dielectric constants, increased reorganization energy, and an elevated entropic barrier for the formation of H_{ad} from H_2O, and, ultimately, reduces the kinetics of the HER/HOR.

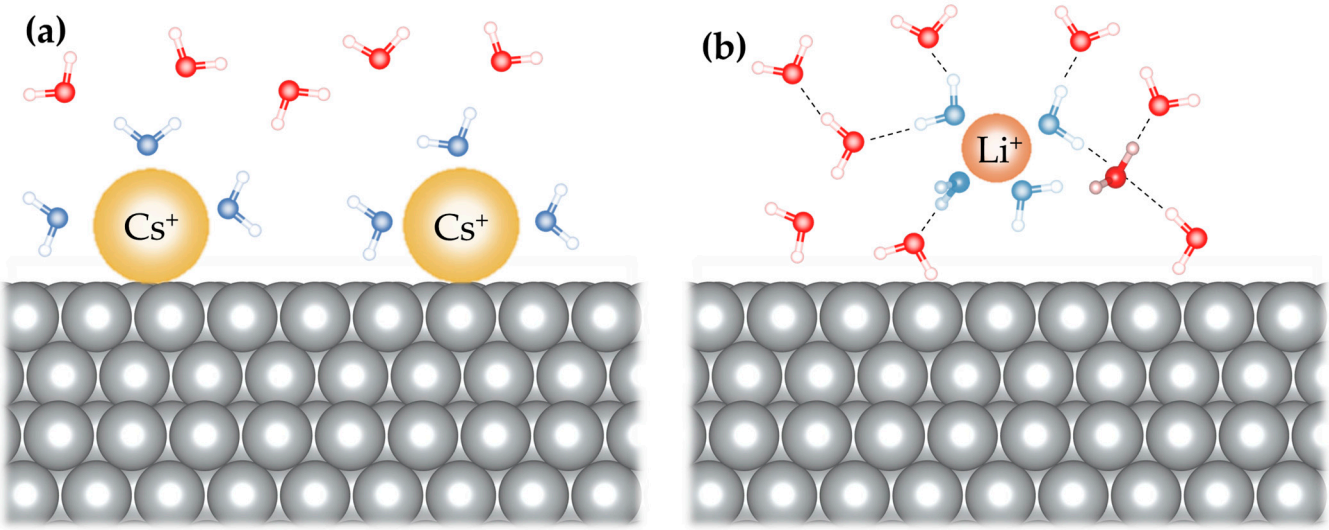

Figure 4. The role of spectator ions, contained in the electrolyte, in modifying the outer Helmholtz layer (OHL) structure of the electrode/electrolyte interface. Schematic illustration (**a**) shows that larger cations (Cs^+) lead to the removal of water molecules from the interface due to strong ion–surface interaction, while (**b**) demonstrating the formation of a stable interfacial water layer with smaller cations (Li+). According to Ref. [111].

Monteiro et al. [112] investigated the influence of cation type and concentration on HER kinetics on Pt and Au electrodes. They found that weakly hydrated cations (e.g., K^+) promoted the HER on gold only at low overpotentials, while strongly hydrated cations (e.g., Li^+) facilitated the HER at higher overpotentials (more alkaline pH). The same pattern was observed for Pt, but weakly hydrated cations inhibited the HER early at lower alkalinity and cation concentrations. Weakly hydrated cations (K^+) are proposed to stabilize the transition state of the water dissociation step since they are more concentrated towards the surface than strongly hydrated cations like Li^+. However, when the pH and, hence, the near-surface cation concentrations are high, the buildup of these species at the outer Helmholtz plane inhibits the HER. This is particularly evident on Pt, where a change in the RDS is shown around pH 13 when employing an electrolyte that contains Li^+ or K^+.

Guha et al. [113,114] conducted an extensive study on how supporting ions like Li^+ can influence the HER activities of metals. They have disclosed that highly-concentrated-electrolyte (sometimes called 'water-in-salt'-type electrolytes)-based catalysis significantly impacts the intrinsic catalytic activity of metals without causing permanent surface alterations. In one of their works, Guha et al. [114] investigated the impact of the Li^+ ion concentration on the HER of polycrystalline Pt and Au. They found that various lithium salts can modify the HER abilities of both materials. Specifically, increasing Li^+ concentration suppresses Pt's HER activity while enhancing it in Au (Table 1). These effects were observed with various counter-ions such as Li^+, Na^+, ClO_4^-, Cl^-, and bis(trifluoromethanesulfonyl)-imide ($TFSI^-$) ions and across different pH conditions (pH 2−13). The effects of the lithium salts, $LiClO_4$, LiCl, and LiTFSI, on the HER process of Au were comparable. An increase in the concentration of $LiClO_4$ from 0.01 to 5 M in 0.01 M $HClO_4$ (pH = 2) and 0.1 M NaOH (pH = 13) has led to a shift in the HER onset potential in the positive direction, indicating the improvement in HER activity. The HER response shows a comparable effect of Li^+ ions on the Au electrode with LiCl and lithium trifluoromethanesulfonate (LiOTf) electrolytes. Conversely, it is demonstrated that LiTFSI suppressed the HER on the Pt electrode, while $LiClO_4$ or LiCl does not affect the HER of Pt. Moreover, the HER activities of Pt and Au were found to be unaffected by Na^+ ions (originating from $NaClO_4$). The authors deduced that the observed variations in the HER catalytic activity are caused by changes in the adsorption energies of various metal ions toward Au and Pt electrodes.

Table 1. Hydrogen concentration and rate of hydrogen formation on Pt and Au electrodes in different electrolytes. Reprinted from Ref. [114]. Copyright 2018 American Chemical Society.

Electrode	Electrolyte	Applied Potential (V vs. Ag/AgCl)	Duration (mins)	Hydrogen Concentrationn (ppm)	Rate of Formation ($\times 10^{-8}$ mol·s^{-1}·cm^{-2})
Pt	0.1 M LiTFSI	−1.1	5	16,550	4056
Pt	20 M LiTFSI	−1.1	5	15,799	3872
Au	0.1 M $LiClO_4$	−1.5	5	5755	2635
Au	5 M $LiClO_4$	−1.5	5	7773	3559
Au	0.1 M LiTFSI	−1.5	5	7950	3640
Au	20 M LiTFSI	−1.5	5	15,577	7132

Additionally, Guha et al. [73] investigated the mechanism behind a tunable HER on various metals at different pH levels using linear sweep voltammetry (LSV), electrochemical impedance spectroscopy (EIS), and Tafel analysis. The study investigated Pt, Ir, Pd, Au, Fe, and Ni catalysts, covering both sides of the Sabatier HER volcano plot, and assessed their HER efficiency under varying Li^+ concentrations. The results revealed that Au, Fe, and Ni exhibited enhanced HER properties with a higher Li^+ concentration, while Pt, Pd, and Ir showed the opposite trend. Moreover, to study the role of anion and LiF formation, the authors have evaluated the effect of different Li^+ concentrations using both LiCl and $LiClO_4$. Similar to the results obtained with LiTFSI, an increase in the Li^+ concentration from 1 M to 5 M (in both $LiClO_4$ and LiCl) has led to HER enhancement on the Au, Fe, and Ni electrodes, while HER suppression was observed on Pt and Ir electrodes. These results offer evidence to support the authors' claim that the suppression of the HER in Pt and Ir is not solely caused by LiF. Figure 5a displays the LSVs for Ir at two different LiTFSI and LiCl concentrations. The authors observed that the suppression of the HER in Pt and Ir with LiTFSI was more significant compared to LiCl and $LiClO_4$. Likewise, for the other metals (Au, Fe, and Ni), the HER enhancement in LiTFSI was lower than in LiCl and $LiClO_4$ (see Figure 5b), indicating the potential formation of LiF, as reported by Suo et al. [78]. The authors confirmed the formation of LiF on the Au, Pt, and Ir electrode surfaces through X-ray photoelectron spectroscopic (XPS) measurements and using attenuated total reflectance Fourier-transform infrared spectroscopy (ATR-FTIR) analyses after the electrolysis. The presence of LiF on the Au electrodes led them to conclude that LiF formation is not the sole reason for the HER suppression with LiTFSI-based aqueous electrolytes, as was previously reported [78]. To verify the effect of Li^+ (using different LiTFSI concentrations) in shifting the H_{UPD} desorption peak of Pt, the authors have also conducted various tests using CVs, LSVs, and EIS in acidic 0.5 M H_2SO_4 (pH = 0) and alkaline 0.1 M NaOH (pH = 13). The CVs of Pt confirm that the HBE of Pt decreased with the increase in the Li^+ concentration in both H_2SO_4 and NaOH electrolytes. The variation in metal HBE of the five metals with varied Li^+ concentrations was also verified by the authors theoretically using DFT and MD studies. Therefore, using theoretical studies, the authors deduced that there is a variation in the metal HBE with changing the Li^+ concentration. At the same time, their experimental results demonstrated variations in the Pt-H and Pd-H binding energies with the Li^+ concentration. Therefore, this study revealed that metals from both sides of the volcano plot can exhibit tunable HER properties, regardless of pH levels (0 and 13) and counter-ions ($TFSI^-$, Cl^-, $ClO_4{}^-$, $NO_3{}^-$, and OH^-), by modifying the M–H bond energy using Li^+ ions.

Another contribution by Guha et al. [113] investigated the use of high-concentration Li^+-ion-containing electrolytes for enhancing the electrocatalytic HER performance of different types of carbon nanotubes (CNTS), namely, metallic multi-wall ones (MWCNTs) and semiconducting single-wall ones (SWCNTs). The outcomes indicated that both the CNTs exhibited an enhancement in their HER performance with the increase in Li^+ ion concentration. To validate the mechanism and establish the significance of Li^+ in improving the HER of the CNTs, the researchers also explored several lithium salts with different counter-ions, such as $TFSI^-$, OTf^-, $ClO_4{}^-$, Cl^-, and OH^-. Interestingly, they observed a

similar enhancement in the HER characteristics of the CNTs. This study suggested that anions play a minor role in the observed phenomenon. Although Suo et al. [78] noted that LiF formation in LiTFSI- and LiOTf-based electrolytes may present a kinetic barrier for proton reduction, higher concentrations of LiTFSI and LiOTf have actually improved the HER performance of the CNTs. Additionally, these electrodes exhibited excellent long-term stability in their HER performance. This study demonstrated that even the slow HER kinetics of CNTs in an alkaline solution can be improved by using an electrolyte-engineering strategy without permanently modifying the surface of the catalyst.

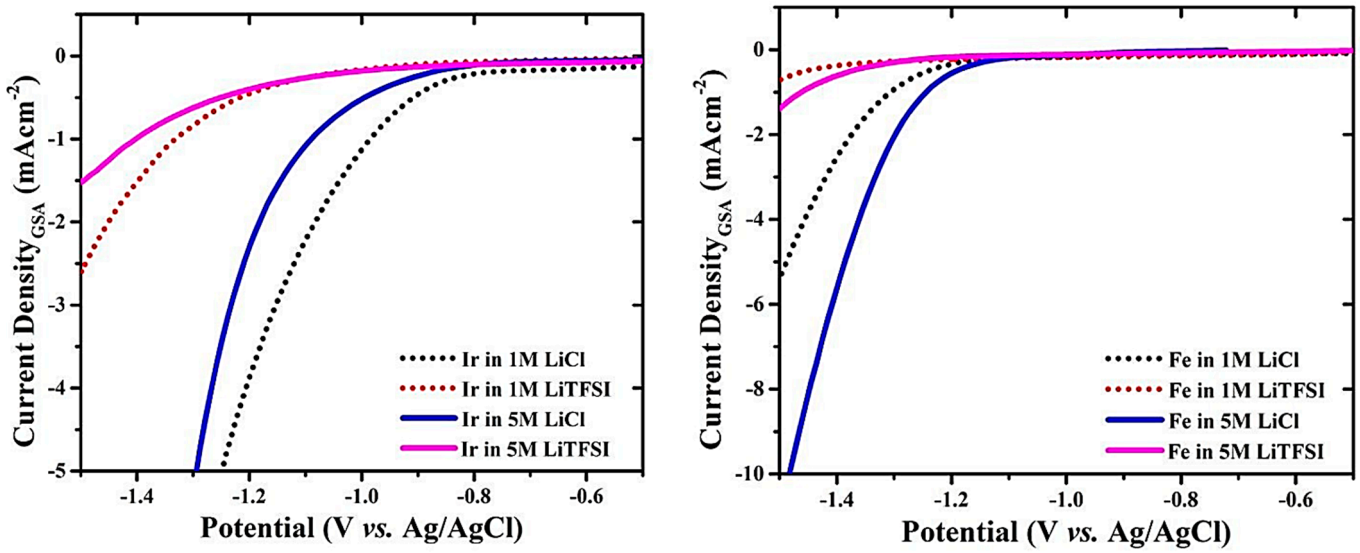

Figure 5. Linear sweep voltammetries of (**a**) Ir and (**b**) Au in two different $LiClO_4$ concentrations. Reproduced from Ref. [73] with permission from the Royal Society of Chemistry.

Comprehending the HER mechanism in bicarbonate electrolytes is vital for CO_2 reduction electrocatalysis, considering the widespread occurrence of bicarbonate in CO_2-saturated solutions and the imperative to inhibit HER activity. As already discussed in Section 2.1, Koper et al. [99] explored the HER in bicarbonate-containing electrolytes on Au and Pt electrodes and observed an increased HER rate with a bicarbonate buffer. Despite the rise in surface pH from water reduction ($2H_2O + 2e^- \rightarrow H_2 + 2OH^-$), bicarbonate is consumed through acid–base reactions and the bicarbonate branch of the HER becomes prominent only with substantial bulk buffer concentrations. Based on this study, the authors deduced that bicarbonate and water reduction seem fundamentally distinct, displaying contrasting reliance on the cation identity and scaling differently with the electrode's specific area. Using microkinetic modeling, the researchers ruled out the explanation of the HER in bicarbonate through proton generation in acid–base reactions. Instead, they proposed a direct bicarbonate reduction pathway, emphasizing its strong dependence on the cation concentration due to the negatively charged reactant.

Koper et al. [115] studied the CO_2 reduction reaction (CO_2RR) on Au electrodes and showed that, without a metal cation, the reaction does not take place in a pure 1 mM H_2SO_4 electrolyte. Moreover, utilizing scanning electrochemical microscopy to study CO_2 reduction and comparing scenarios with and without metal cations, they found that CO is exclusively generated on the Au, Ag, or Cu electrodes when a metal cation is present in the electrolyte. Through DFT simulations, the authors presented conclusive evidence that positively charged species from the electrolyte play a crucial role in stabilizing the key reaction intermediate. In another contribution, Koper et al. [116] utilized rotating ring disc electrode (RRDE) voltammetry to assess how bicarbonate and cation concentrations influence CO_2RR and HER currents on an Au disk, impacting the Faradaic efficiency to

CO (FE(CO)). By varying the bicarbonate and cation concentrations and adjusting rotation rates, the authors uncovered two distinct potential regimes for electrolyte effects. These regimes were characterized by an opposite interplay of CO_2RR and the HER kinetics. In the first regime (low negative potential), higher HCO_3^- and Na^+ concentrations enhance FE(CO). Conversely, in the second regime (more negative potential), lower HCO_3^- and Na^+ concentrations are preferred to suppress the HER. This study provides in-depth insights into the impact of electrolyte composition and mass transport, aiding in defining the optimized electrolyte conditions for achieving a high FE(CO). Interested readers are recommended to explore a brief review on the effects of electrolytes on CO_2RR by Koper et al. [117]. The review highlights the crucial role of cations in co-ordinating and stabilizing the initial electron transfer intermediate, CO_2^-, in the CO_2 reduction to CO. The kinetics of the reaction are significantly influenced by the cation's characteristics, including the hydration number and acidity. For optimal performance, the study suggests using weakly hydrated alkali cations like Cs^+ or K^+ to achieve a high current density regardless of the pH, while intermediate cation concentrations ($\leq$0.1 M) are preferred due to their promotion of concomitant water and bicarbonate reduction. In a more recent study, Koper's group [118] explored the impact of cations on HCOOH and CO formation during CO_2RR on Pd_{ML}Pt-(111) in pH 3 electrolytes. The absence of metal cations resulted in the formation of only a small amount of adsorbed CO, while increasing cation concentrations led to a decrease in the onset potential of HCOOH and CO. Using DFT simulations, the study uncovered that the formation pathways of both CO and HCOOH involve negatively charged intermediates, such as negatively charged adsorbed CO_2 and adsorbed hydride, whose formation is enhanced by interactions with cations.

In the context of electrolyte and cation effects on electrocatalysis, it is important to mention the study of Strmcnik et al. [106], who explored how Li^+, Ba^{2+}, and K^+ impact Pt and Au during the ORR in an alkaline solution. They observed that, in an alkaline environment, Li^+ had a strong interaction with adsorbed OH^- ions at the active sites of the Pt surface, leading to the blocking of these active sites for the ORR on Pt. Therefore, the presence of Li^+ results in a decrease in the ORR activity of the Pt surface. However, this effect was not observed on the Au surface due to the small coverage of OH^- ions on the Au surface. A DFT study conducted by Matanović et al. [119] provides additional evidence, indicating that, when H^+ ions are present at low concentrations, alkali metal ions compete with them for adsorption on the Pt surface, blocking the active sites on the Pt surface and suppressing the HER. As the Li^+ concentration rises, the H^+ concentration falls relative to the Li^+ concentration, creating strong competition between Li^+ and H^+ for adsorption on the Pt surface [78]. The effect of alkali metal cations (originating from $MClO_4$, where M refers to Li^+, Na^+, K^+, Rb^+, or Cs^+) on the electric double layer (EDL) capacitance of Pt(111) and Au(111) electrodes was investigated by Garlyyev et al. [120]. The study revealed that the local effective concentrations of cations near the electrode for both Pt(111) and Au(111) electrodes can reach ~80 times higher than those in the bulk solution. The EDL capacitance increased linearly $Li^+ < Na^+ < K^+ < Rb^+ < Cs^+$, indicating a significantly higher effective Li^+ concentration within the double layer compared to the bulk solution. Another DFT-based theoretical work [121] revealed that Pt has a greater affinity to Li^+ ions compared to Au. According to the DFT calculations, the adsorption potential of Li^+ on the surfaces of Pt and Au is -1.30 V and -2.76 V vs. NHE, respectively. As a result, the strongly adsorbed Li^+ ions block the active sites of Pt, hindering the HER. Additionally, Li^+ has the capacity to destabilize water molecules [46], and the high Li^+ concentration near the electrode surface may be favoring the breakdown of water molecules, which would then result in increased the HER activity of Au where the surface is not obstructed by Li^+ ions.

In our recent work [55], we have investigated the effect of the nature of the electrolyte (0.1 M $HClO_4$, 0.1 M HCl, 0.5 M NaCl, 1 M KH_2PO_4, 0.1 M KOH, 1 M KOH, and 0.1 M LiOH) on the HER activity of various monometallic polycrystalline electrodes (Pt, Ni, W, Co, Fe, Cr, Ag, Au, and Zn), both for freshly polished and oxidatively treated electrodes. In order to compare the HER catalytic activities of the investigated metals in the various

electrolytes, we have determined the overpotential values required to achieve a current density of -0.1 mA cm^{-2}_{real} ($\eta_{0.1,real}$). The HER activity of the metals in the investigated electrolyte solutions, as determined by the $\eta_{0.1,real}$, follows the following order: 0.1 M $HClO_4$ > 0.1 M LiOH > 1 M KH_2PO_4 > 0.1 M HCl > 1 M KOH > 0.1M KOH > 0.5 M NaCl. The HER of the metals in LiOH was remarkably high, which is attributed to the effect of the Li ions [111,122]. The higher HER activity of metals in a 1 M KH_2PO_4 solution can be attributed to the effect of K^+ ions, the buffering properties of KH_2PO_4, and the involvement of weak acid components ($H_2PO_4^-$ and HPO_4^{2-}) in the reduction process, as suggested by previous studies [71,94,100]. It is widely accepted that the accelerated formation of H_{ads} intermediates from H_3O^+ significantly enhances the HER activity of metals in the acidic solutions (0.1 M $HClO_4$ and 0.1 M HCl). While the higher activity of the metals in 0.1 M $HClO_4$ can be ascribed to the non-adsorbing property of the ClO_4^- anion [75], conversely, the decreased activity of the metals in the HCl and NaCl solutions can be attributed to the negative effects of Cl^- ion poisoning. The higher HER activity of the metals in 1 M KOH compared to 0.1 M KOH is primarily due to the concentration effect of K^+ ions [123].

There are conflicting views on the influence of electrolyte anions on the HER. Some studies suggest their effect is insignificant, as already exemplified, while others reveal that electrolytes can significantly influence the HER of metal catalysts. A comparable HER/HOR performance of Pt across three electrolytes ($HClO_4$, HNO_3, and H_2SO_4) is reported in Ref. [124]. Moreover, Ref. [125] shows that, in contrast to the HOR, the HER current densities, which have been examined in low overpotential and underpotential sites, were found to be independent of the nature of the supporting electrolyte ($HClO_4$, H_2SO_4, and HCl). Similar HOR/HER activities in the presence of $H_2SO_4^-$ and $HClO_4^-$ ions were reported, which could be possibly because these counter-anions may not adsorb on the catalyst surface at HOR/HER-relevant potentials in the vicinity of ≈ 0 V_{RHE} [80]. Moreover, as already discussed, Guha et al. [113] revealed that the effect of the nature of anions ($TFSI^-$, OTf^-, ClO_4^-, Cl^-, and OH^-) on the HER of the CNTs was minor.

Several studies have explored how strong anion adsorption on PGM surfaces influences the kinetics of pseudo-capacitive and Faradic processes. Anions can also adsorb on the electrode surface at potentials below the potential of zero charge, particularly within the H_{UPD} region, impacting Pt-H_{ad} energetics and potentially causing alterations in the HER kinetics [80]. In practical terms, anionic contamination from SO_3^- ions, which may be released during polymer electrolyte membrane degradation in electrolyzer/fuel cell operation, could adversely affect device performance and durability, especially with ultra-low PGM loadings. Furthermore, the presence of Br^- and I^- were reported to significantly reduce the overall rates of the HER/HOR [80].

As already mentioned, our recent study [55] revealed the effect of both cations and anions on the HER of different metals. More specifically, the impact of Cl^- ions was significant in both 0.1 M HCl and 0.5 M NaCl. This effect was evident on the volcano plots (a plot of the HER overpotential values needed for the current density of 0.1 mA cm^{-2}_{real}, vs. the DFT-calculated HBE) (Figures 6 and 7). One can easily observe the impact of the electrolyte on the shape of the volcano curve, as evidenced by the broader overpotential range (from ~0 to >-0.6 V) required for the HER in HCl (Figure 6b) compared to $HClO_4$ (Figure 6a), which can be attributed to the Cl^- ion poisoning in 0.1 M HCl and the non-adsorbing property of the ClO_4^- anion in 0.1 M $HClO_4$. The effect of electrolytes is also noticeable in neutral solutions, with NaCl (Figure 7a) exhibiting higher HER overpotentials than KH_2PO_4 (Figure 7b). Moreover, the volcano peak shifts by approximately -0.3 V, and unique characteristics such as flattened trends for W and Cr are observed in the NaCl solution. At the same time, Co exhibits unexpectedly low activities in both the pH-neutral solutions investigated. These findings align with the concepts proposed in Ref. [126], which discuss the activity of metals with highly exothermic hydrogen adsorption. The effect of SO_4^{2-} and ClO_4^- anions on the HER activity of Pt(110) in 0.1 M KOH was examined by Sheng et al. [75]. ClO_4^- was shown not to affect the HBE, while the addition of SO_4^{2-} slightly altered the HBE of Pt(110).

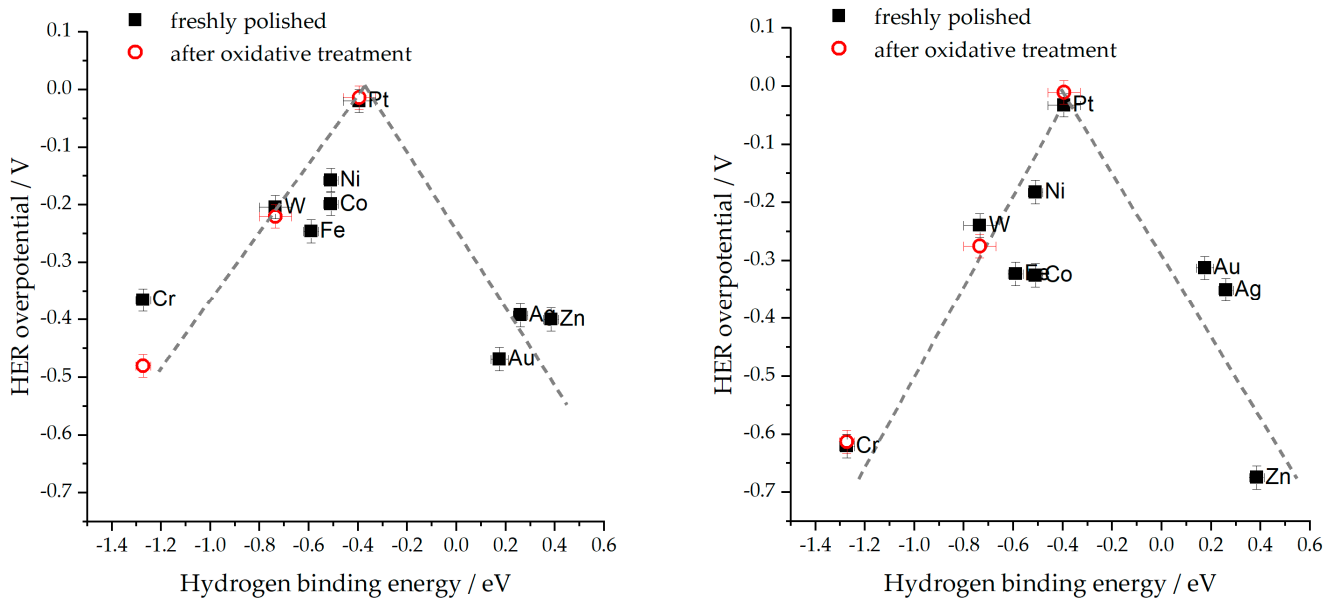

Figure 6. The HER volcanoes in acidic solutions: (**a**) 0.1 M $HClO_4$; and (**b**) 0.1 M HCl. Freshly polished electrodes are represented by squares, and circles are used to represent electrodes after undergoing oxidative treatment. Reproduced from Ref [55]. This work is an open-access article distributed under the terms and conditions of the Creative Commons Attribution (CC BY).

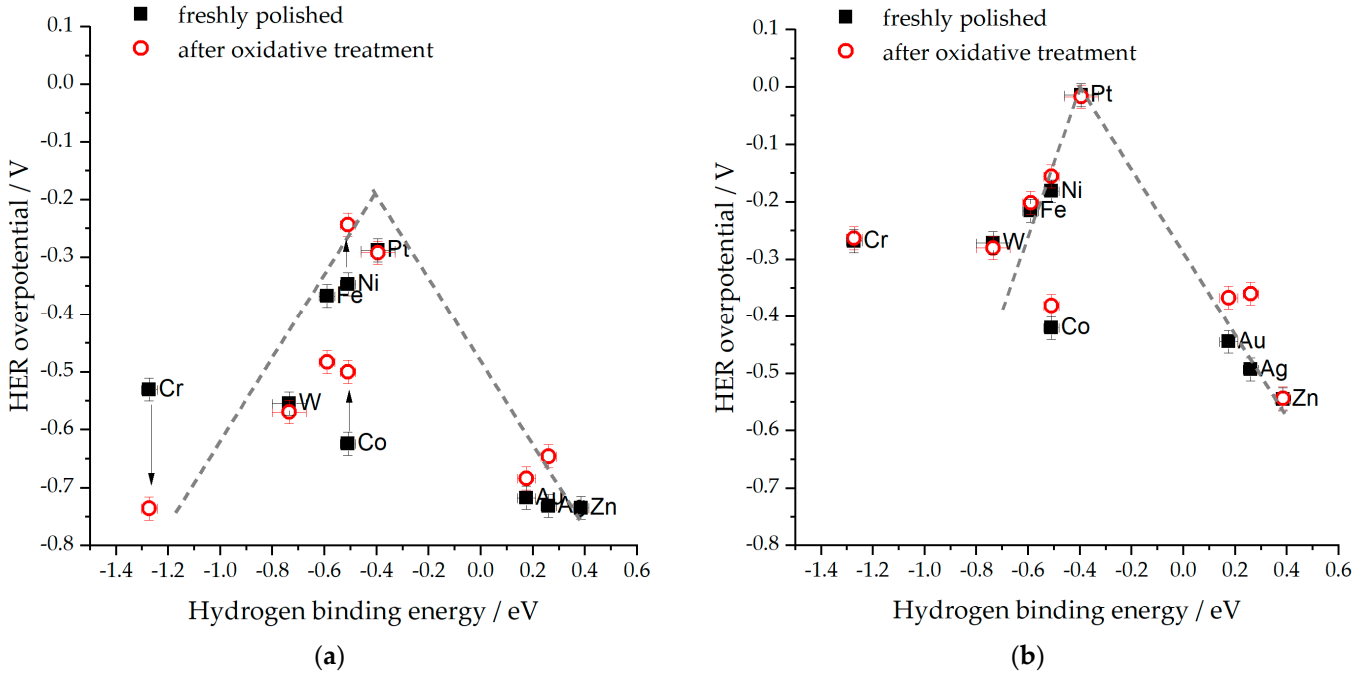

Figure 7. The HER volcanoes in neutral solutions: (**a**) 0.5 M NaCl (simulated sea water); and (**b**) 1 M KH_2PO_4 (pH was adjusted to 7.0 in both electrolytes). Freshly polished electrodes are represented by squares, and circles are used to represent electrodes after undergoing oxidative treatment. Regarding the NaCl solution, significant changes in activity are indicated by arrows. Reproduced from [55]. This work is an open-access article distributed under the terms and conditions of the Creative Commons Attribution (CC BY).

Seawater electrolysis, a key process for green hydrogen production, encounters many challenges, including the concentration overpotential and *iR* drop [3]. Aiming to enhance

the efficiency of seawater electrolysis, a recent study by [127] introduced a novel mixed buffer electrolyte with a 1:1 borate/carbonate molar ratio with a new apparent pK_a ($pK_{a,app}$) of pH 9.8. The electrolyte deliberately incorporates concentrated Cl^-, achieving a conductivity of about 50 S m^{-1} at 353 K, which is on par with 30 wt % KOH (~130 S m^{-1}). The mixed buffer electrolyte with Cl^- optimizes the hydrogen and oxygen evolution reactions using $RuNiO_xH_y$/Ni felt and $CoFeO_xH_y$/Ti felt, respectively. Through electrolyte engineering, cation concentration tuning, and pH adjustment, a zero-gap cell was achieved, operating stably at 2.00 V and 500 mA cm^{-2} for 80 h with minimal *iR* loss. This design showcases an innovative approach to seawater splitting for enhanced electrolytic performance.

2.3. Electrolyte Concentration and HER Kinetics

Arminio-Ravelo et al. [128] studied the effect of electrolyte composition and concentration on commercial Ir black nanoparticles using varying concentrations (0.05 M, 0.1 M, and 0.5 M) of H_2SO_4 and $HClO_4$. It was found that H_2SO_4 hindered Ir oxidation and catalyst performance, while $HClO_4$ showed minimal interference and a better catalytic performance than H_2SO_4, regardless of its concentration. Varying concentrations of $HClO_4$ showed no significant impact while an increasing H_2SO_4 concentration led to decreased activity due to the stronger adsorption of HSO_4^- and SO_4^{2-} anions on the catalyst surface compared to ClO_4^- anions. $HClO_4$ is suitable for catalytic performance as it has minimal impact, but concentrations higher than 0.1 M should be avoided to prevent potential anion interactions. The authors recommend using $HClO_4$ as the electrolyte for benchmarking and reporting activity and stability trends in the RDE measurements of Ir-based materials.

The effect of the nature of the electrode (polycrystalline and nanostructured), pH (12 to 14), and concentration of the electrolyte (0.01 to 2 M KOH) on the HER activity of Ni-based catalysts was investigated by Faid et al. [129]. The findings showed that a pH and KOH concentration variation influenced the HER activity by affecting the ECSA and Tafel slope. The nanostructured NiMo catalyst exhibited an enhanced HER activity, and the Tafel slope was reduced from ~−180 mV dec^{-1} to −60 mV dec^{-1} in the pH range of 12–14 and KOH concentrations of 0.01–1.0 M, indicating a promoting region for both the ECSA and reaction order. Polycrystalline Ni showed different behaviors in different pH and KOH concentration regions, maintaining Tafel slopes around −120 mV dec^{-1}. However, both catalysts' HER performances were inhibited under the conditions of decreased OH_{ad} transport kinetics. The higher HER activity of various metals in 1 M KOH than in 0.1 M KOH was also observed in our recent work [55]. Moreover, Li et al. [130] observed that the HER activity of Pt(pc) was improved with the increase in NaOH concentration from 0.01 M (pH 12) to 1.0 M (pH 14). Kuznetsov et al. [131] observed that the anodic charge and ECSA of NiCu/C catalysts were influenced by the NaOH concentration. They also found that the HER activity of a partially oxidized Ni disc electrode improved with increasing pH/NaOH concentrations when the potential was below −0.18 V vs. RHE. Moreover, current densities in cyclic voltammograms were found to vary with changes in the electrolyte concentration, resulting in variations in the apparent ECSA of Ni nanostructures [132]. Goyal et al. [123] investigated the impact of the electrolyte pH and alkali metal cation concentration on the HER kinetics on Au electrodes. They found that increasing the cation concentration significantly enhances the HER activity at a moderately alkaline pH (pH = 11) by accelerating the sluggish Volmer step. It is highlighted that the electrolyte pH and bulk cation concentration affect the surface cation concentration and influence the water dissociation kinetics, with interfacial cations stabilizing the transition states. Yet, excess near-surface cations, particularly at elevated pH and cation levels, can impede HER activity by obstructing active sites.

Furthermore, studies indicate that optimizing the electrolyte composition can significantly enhance mass transport and improve the efficiency of the HER, particularly when operating at near-neutral pH conditions [92,133]. Shinagawa et al. [94] studied, both experimentally and theoretically, the effect of the electrolyte concentration on the Pt electrode under neutral-buffered conditions, employing sodium phosphate (0.2–4.2 M at pH 5) as the

electrolyte solution. Both experimental and theoretical research revealed a volcano-shaped relationship between the solute concentration and HER activity. The HER performance increased with solute concentrations up to 2 M, but higher concentrations resulted in decreased performance. Their microkinetic model combined with a description of mass transport closely matched the experimental results, indicating the presence of notable concentration overpotentials during the HER under buffered-neutral conditions. Their simulation model indicated that the concentration overpotential surpassed 46% even at 0.5 M, while the kinetic overpotential remains the lowest (~10%) due to sluggish mass transport. The authors emphasized that mass transport is influenced by diffusion and activity coefficients, with the former determined by ion size and electrolyte viscosity. Thus, adjusting these parameters through effective electrolyte engineering can significantly enhance HER performance in neutral conditions, regardless of the electrocatalyst used.

During water splitting, oxygen is evolved at the anode (OER) and can migrate to the cathode, where catalysts for the HER also facilitate the oxygen reduction reaction (ORR). Oxygen crossover between the anode and cathode in membraneless cells reduces the HER efficiency due to undesired competitive reactions, underscoring the need for an oxygen-tolerant HER to improve efficiency. Shinagawa et al. [92] found that selecting the proper electrolyte enhances cell efficiency by controlling the mass transport of oxygen and the proton source (for example, weak acid). The study extensively analyzed the influence of different solutes on the HER and ORR under heavily-buffered conditions. They tested various electrolyte solutions, including KH_2PO_4, K_2HPO_4, K_3PO_4, LiH_2PO_4, NaH_2PO_4, $NaHCO_3$, $HClO_4$, and KOH, and mixtures of them, in the concentration range of 0.01 to 3.0 M. Under specific conditions (1.5 M NaH_2PO_4 or 1.5 M 40% K_2HPO_4 + 60% KH_2PO_4), the overpotential required to achieve -10 mA cm^{-2} was found to be less than -40 mV with a 90% selectivity towards the HER in oxygen-saturated electrocatalytic conditions (Figure 8). Using such highly concentrated buffers also reduced solution resistance, further enhancing the overall HER performance. The existing literature highlights that the concentration of electrolytes plays a crucial role in the electrocatalytic HER, having a positive impact up to a certain threshold level, beyond which it adversely affects the HER.

2.4. Effect of Electrolyte Impurities

Electrolyte impurities can substantially impact the HER kinetics, causing the reduced efficiency or complete inhibition of the reaction. Common impurities found in the electrolyte are metal ions, organic contaminants, and other foreign substances, which can modify the electrode's surface properties, affect the reaction kinetics, and cause undesired side reactions during the HER. Impurities in electrolysis cells can originate from various sources. For instance, commercial KOH electrolytes may contain Zn as an impurity [6], while Pt and Au counter-electrodes used in measurements can also introduce contaminants [80]. Moreover, impurities can arise from corrosion products of cell components due to the corrosive environment caused by highly alkaline electrolytes, high temperature, and the presence of molecular oxygen [134]. The HER activity of surfaces with low j_0 values can be influenced by trace metal cations in the electrolyte, which can plate onto the surface due to the HER starting at low potentials [80]. Impurities can deposit as metallic species during H_2 production through cathodic reduction or as salts/hydroxides through chemical precipitation, causing the passivation of catalytically active sites [134]. Weber et al. [135] investigated the challenges in benchmarking the HER/HOR activity of Pt-based catalysts in alkaline media, viz., 0.1 M LiOH, NaOH, and KOH. They analyzed the electrochemical setup (such as the cell material, hydrogen gas, and electrolyte solutions) to identify the source of the impurities. They identified glass cells and hydrogen gas as non-significant sources of contamination. However, they noticed a significant reduction in the ECSA of Pt following HER/HOR measurements, especially in 0.1 M NaOH and LiOH solutions. Through long-term chronoamperometric experiments and X-ray photoelectron spectroscopy analysis, the authors discovered that trace metals (Cu, Zn, Pb, and Fe) from electrolyte salts were deposited on the Pt surface during the HER.

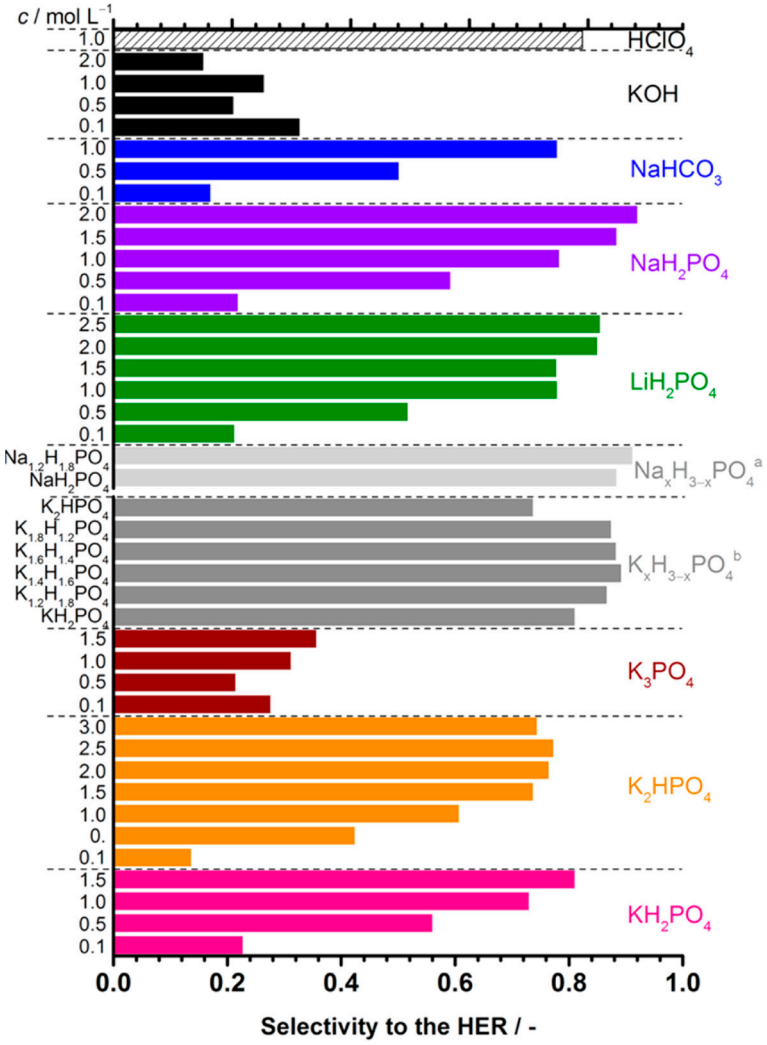

Figure 8. Calculated Faradaic efficiency to the HER in various electrolyte solutions using a polycrystalline Pt disk electrode.Reprinted with permission from Ref. [92]. Copyright (2016) American Chemical Society.

Studies show that the presence of trace metal cations can have both positive and negative effects on the HER activity of the substrate metal [80]. Li et al. [136] studied the influence of trace iron impurities and alkali metal cations (Na^+ and Cs^+) on the HER of polycrystalline Cu electrodes in alkaline conditions. The study found that, during electrolysis in 0.1 M solutions of NaOH and CsOH, with the highest commercially available purity grades, small amounts of iron impurities were deposited on the Cu electrode. The presence of iron impurities significantly accelerated the HER rate in 0.1 M CsOH by up to five times over eleven CVs. The authors have pre-electrolyzed the electrolyte solution to remove iron impurities effectively, and, after removing the iron impurities, the CVs stabilized with the cycle number. For purified electrolytes (0.1 M NaOH and CsOH), the HER current densities were found to be nearly identical, suggesting no significant cation effect on the HER rate on Cu. Similar findings are reported for other electrocatalytic reactions, like the OER. Klaus et al. [137] studied the influence of Fe incorporation on the structure–activity relationships in Ni-(oxy)hydroxide by analyzing aged $Ni(OH)_2$/NiOOH films in KOH using various characterization techniques. They discovered that aging in unpurified KOH led to a >20% Fe incorporation after five weeks, resulting in a higher OER activity, lower overpotential, and lower Tafel slope compared to samples aged in Fe-free KOH. Optimal catalyst activity was observed with five-day aging in unpurified 1 M KOH. Salmanion et al. [138] explored the OER of Co and Au in Ni- and Fe-free KOH.

The results demonstrated that cobalt oxide served as a relatively efficient catalyst for the OER in a pure electrolyte, while gold does not exhibit good catalytic activity under the same conditions. Iron impurities in the form of FeO_2^- present in commercial 1.0 M KOH electrolytes are actually known to react with Au electrode surfaces and create active sites for the OER [139]. Moreover, Gong et al. [140] reported that Fe had a synergistic effect with Co, Ni, Cu, Ag, and Au (but not Ti) in enhancing the OER. Although the Co electrode showed good OER catalytic activity in a pure electrolyte, its Tafel slope decreased significantly in the presence of Ni-containing (Fe-free) KOH [138]. The study suggests that Ni ions precipitate on the electrode's surface, altering the redox-active sites, emphasizing the significance of trace electrolyte impurities and proposing the use of pure electrolytes for evaluating the electrocatalysts' performance for the OER. Extensive research has explored how arsenic compounds affect the HER and H_{UPD} on Pt, Ni, and steel electrodes. Even trace amounts of arsenic (~10^{-8} M) were consistently found to reduce j_0 and increase he overpotential for the HER [141–143].

Moreover, both PEMEL and AEL cells can have two types of impurities: exogenous and endogenous. Electrolyzers usually need highly purified water, but the purified water may still contain low concentrations of ionic species and total organic carbon, considered as exogenous impurities [144]. The growing adoption of green hydrogen technology may raise the pure water demand, thus creating public concerns in water-scarce areas. Re-using purified wastewater could address this, but it is energy-intensive and expensive. Opting out of proper purification for industrial processes risks contaminating electrocatalysts with impurities from untreated water [1]. Endogenous impurities in electrolyzer systems, on the other hand, originate from internal sources. Throughout its operation, electrolyzers may undergo a gradual deterioration of their stack and balance of plant (BoP) parts, resulting in the production of impurities within the system. Additionally, impurities may arise from component leaching and contamination during the electrolyzer manufacturing, commissioning, and maintenance processes. Cations in PEMWEs present significant challenges as impurities, impacting the catalyst, ionomer, and membrane. Their presence can lead to performance degradation and a reduced lifespan, as depicted in Figure 9. Anions are often associated with initiating side reactions, such as chlorine evolution, potentially affecting the hydrogen quality and accelerating corrosion in metallic components [144]. In contrast to cations, anions cannot replace protons within the membrane and ionomer, leading to different operational mechanisms (Figure 5).

Therefore, to achieve the best HER performance, it is crucial to use high-purity electrolytes and meticulously control their quality to minimize the influence of impurities. Studies revealed that shielding the counter-electrode and pre-treating the electrolyte can help minimize the impact of metal cation impurities on the HER. Moreover, an electrochemical purification step aimed at diminishing impurities originating from the electrolyte solution was devised by Weber et al. [135], which demonstrated that pre-electrolyzing the electrolyte solutions was found to be effective in removing iron impurities. The use of self-assembling and self-healing catalytically active films to overcome the cathode deactivation triggered by electrolyte impurities is also mentioned in Ref. [134]. According to this study, introducing a trace metal impurity (Zn) has raised the cell voltage. At the same time, adding an active material (Ni_xB) formed a self-assembled catalyst film, restoring activity and lowering the voltage. To mitigate catalyst poisoning, using more resistant catalysts is an option. Metal-oxide-based catalysts are less susceptible to poisoning compared to unmodified ones. Catalysts with carbonate, sulfate, and oxide compounds also display enhanced resilience against deactivation. For instance, the MoS_2 electrocatalyst was found to be more tolerant to sulfur poisoning than Pt/C [1]. Carbon-based materials like nanotubes or graphene can also mitigate contaminant effects by serving as active HER electrodes. Despite lacking inherent strong catalytic properties, these materials can be modified with small catalyst amounts for highly efficient electrocatalysis. Doping graphene with heteroelements like nitrogen, sulfur, phosphorus, or boron enhances its electrocatalytic

performance. Modified electrodes also display a remarkable resistance to surface poisoning; intriguingly, impurities might improve their catalytic capabilities [145–147].

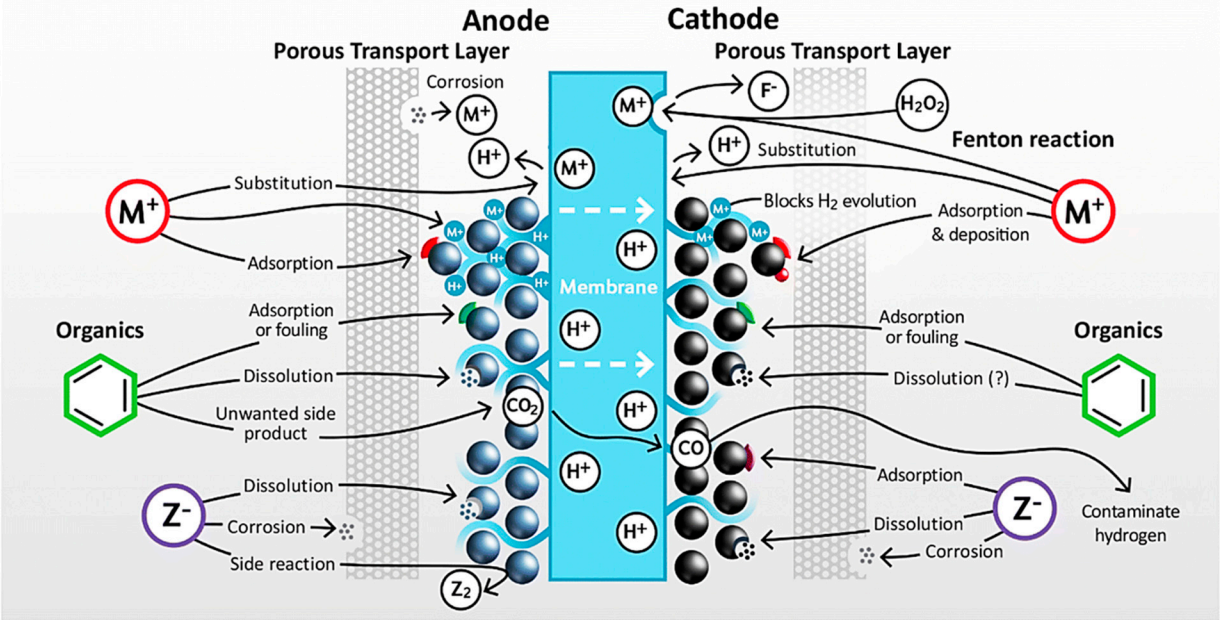

Figure 9. Diagrammatic representation of the impact of different types of impurities on PEMWEs. Reproduced from Ref. [144]. with permission from the Royal Society of Chemistry.

Besides PEMEL technology, other important water electrolysis approaches are also impacted by the properties of the electrolyte. These include the standard alkaline water electrolyzer (AWE), anion exchange membrane electrolyzer (AEME), solid oxide electrolysis cell (SOEC), and protonic ceramic electrolysis cell (PCEC) approaches [11]. AWE is absolutely the most mature among them, typically employing 5–7 mol dm^{-3} KOH as the solution. On the other hand, AEME is rapidly developing and has several advantages over classical AWE, like higher current densities and a higher purity of produced gases. Considering AWE and AEME, the impact of the electrolyte composition and impurities can be regarded from the fundamental aspect, focusing on the specific interactions at the electrode interface, as discussed earlier. For example, one of the advantages of AEME over AWE is higher voltage efficiency which is partially due to the milder alkaline environment (1 mol dm^{-3} KOH). However, the electrolytes also affect the overall performance of an electrolyzer system through their conductivity (causing Ohmic losses), viscosity, solubility of gases, and other, more technical, aspects.

3. Summary and Outlook

This review explores the impact of electrolytes on hydrogen evolution reaction (HER) kinetics, emphasizing the pH, cations, anions, and impurities. It briefly covers how the electrolyte concentration affects HER kinetics, highlighting its beneficial impact up to a certain level, beyond which it hampers efficiency. The electrolyte pH significantly influences the HER by altering the catalyst–electrolyte chemistry and proton concentrations, affecting metal's hydrogen binding energy, proton donor, water adsorption, and interfacial water reorganization. These factors collectively determine the reaction kinetics, catalyst effectiveness, and overall HER efficiency. Although there are differing opinions, there is a general consensus that the HER activity tends to decrease with higher pH levels. Yet, the HER behavior in neutral solutions presents a unique phenomenon. Conversely, neutral solutions allow for applications such as seawater utilization and eliminate the need for specialized materials or acid/alkali-resistant catalysts. The pH-neutral HER is affected by reactant properties, electrolyte state (buffered/unbuffered), and concentrations. The insufficient

H_3O^+ ions restrict the HER activity in pH-neutral solutions at the electrode–electrolyte interface, but buffering enhances the H_3O^+ supply. Additionally, studies suggest weak acids like phosphate species ($H_2PO_4^-$ and HPO_4^{2-}) likely act as reactants under buffered conditions. In water splitting, oxygen evolved at the anode (OER) can cross to the cathode in membraneless cells, affecting the HER. For this purpose, heavily buffered electrolytes are found to exhibit better HER performance with very high selectivity towards the HER in oxygen-saturated electrocatalytic conditions regulating the oxygen transport and proton source (for example, weak acid).

Beyond the electrolyte pH, electrolyte ions are also known to impact the kinetics of the HER. Spectator ions can influence HER kinetics by co-adsorbing or interacting with adsorbed intermediates on catalyst surfaces. Recent studies show that aqueous electrolytes with Li+ can effectively enhance various electrochemical reactions, including the HER. Notably, a ~4-times HER performance difference is observed between Li^+- and Cs^+-containing electrolytes. Electrolytes with larger (more structure-breaking) cations exhibit more surface-bound cations than smaller (more structure-making) ones, influencing the interfacial hydrogen-bonding network and solvent reorganization energy. Larger cations like Cs^+ remove water molecules at the interface through a strong ion–surface interaction, while smaller cations like Li^+ create a stable interfacial water layer. An optimal Li^+ ion concentration improves the HER on noble metals (such as Au) but affects the HER on platinum group metals (PGMs) (such as Pt, Ir, and Pd) less favorably. Pt has a greater affinity towards Li^+ ions compared to Au, and, thus, strongly adsorbed Li+ ions can block active sites of the Pt surface. In contrast, a high Li^+ concentration near the electrode boosts the breakdown of water, increasing the HER in unobstructed Au surfaces. These observations indicate that manipulating the electrolyte composition offers the potential for modifying noncovalent interactions and solvation dynamics at the electrified interface, which could result in notable alterations in catalytic activity and selectivity.

The impact of electrolyte anions on the HER is debated; some studies find them negligible, while others emphasize their substantial influence on the kinetics of the HER. Anions can also adsorb on the electrode surface at potentials below the potential of zero charge, especially in the H underpotential (H_{UPD}) region, affecting the M–H_{ad} energetics and potentially reshaping the HER kinetics. Sulphate (HSO_4^- and SO_4^{2-}) and chloride (Cl^-) ions are known to affect the HER negatively. Conversely, $HClO_4$ is suggested as an ideal electrolyte for benchmarking and reporting activity and stability trends in rotating disk electrode (RDE) measurements due to the neutral or beneficial impact of ClO_4^- anions on HER kinetics. Anionic contamination from SO_3^- molecules during polymer electrolyte membrane degradation is also known to negatively impact device performance and the durability of electrolyzers, particularly at low PGM loadings.

Electrolyte impurities can also substantially impact the HER. Impurities can arise from multiple origins: from commercial electrolytes (e.g., Zn in KOH), or from Pt and Au counter-electrodes. Additionally, impurities can result from corrosion products due to a corrosive electrochemical environment. Proton exchange membrane electrolysis and alkaline electrolysis cells can contain two impurity types: exogenous and endogenous. While electrolyzers require purified water, they may still contain slight levels of ionic species and organic carbon as exogenous impurities. In industrial-scale operations, compromising water quality and chemical selection can pollute electrocatalysts, posing a notable catalyst deactivation challenge. On the other hand, endogenous impurities stem from internal sources, often arising from gradual system deterioration and leaching in components. Although some studies highlight the positive impact of trace metal impurities on the HER activity of the substrate metal, electrolyte impurities are known to modify electrode surfaces, affect reaction kinetics, and trigger undesired side reactions during the HER. Therefore, for optimal HER performance, utilizing high-purity electrolytes and rigorous quality control to minimize the impacts of impurities is essential. Moreover, employing pure electrolytes when assessing electrocatalyst performance is sensible, as impurities can either enhance or diminish the catalyst efficiency. Research suggests techniques such

as electrolyte pre-treatment, electrochemical purification, shielding of counter-electrodes, and self-assembling and self-healing catalytically active films to mitigate the influence of impurities.

Clearly, depicting a comprehensive view of the electrolyte effects on HER kinetics is a difficult, if not impossible, task. However, it seems that a critical mass of fundamental knowledge has been acquired, and optimizing electrolytes looks like a tangible approach to boosting HER activity in the context of green hydrogen production. In fact, this could be the most straightforward approach to increase the efficiency of existing electrolyzer systems, as replacing electrolytes does not require a disruptive technology shift, while it can lead to significant improvements in the efficiency of the water electrolysis process. The available literature sources suggest a possible path towards achieving this goal. Namely, it seems that a careful electrolyte optimization in terms of the concentration of structure-making and structure-breaking cations (depending on the current densities that will be applied), the use of anions that do not specifically adsorb and poison the catalyst surface, and the rigorous control of the presence of impurities that have a detrimental effect on the activity could be a viable route.

Nevertheless, to reach the mentioned goal, the anode side must be investigated as well. That is, the electrolyte effects on the OER should be addressed, too. However, the OER is a much more complex reaction than the HER. Here, we have mentioned several examples of electrolyte effects on oxygen electrode reactions (both ORRs and OERs). Moreover, the OER conditions are much harsher than the HER conditions. Thus, structural and chemical changes in the anode can also induce electrolyte concentration and composition changes in the interfacial region [148]. Due to its complexity, a comprehensive view of electrolyte effects on the oxygen electrode can remain elusive for a long time. However, this fact should not discourage future research in electrolyte engineering for improved water electrolysis efficiency.

Finally, we note that the majority of experimental work on the electrolyte effects on HER kinetics has been carried out using metallic electrodes. However, other types of HER catalysts are actively investigated these days. Thus, a systematic analysis is also needed for these materials, like carbon-based catalysts, sulfides, phosphides, nitrides, and others. Moreover, the electrolyte effect could be particularly important in the case of single-atom catalysts, and the community should delve into these important questions.

Author Contributions: Conceptualization, I.A.P. and G.K.G.; validation, I.A.P.; investigation, G.K.G. and A.Z.J.; writing—original draft preparation, G.K.G. and A.Z.J.; writing—review and editing, I.A.P.; visualization, G.K.G.; super-vision, I.A.P.; funding acquisition, I.A.P. All authors have read and agreed to the published version of the manuscript.

Funding: This research was funded by the Serbian Science Fund, grant RatioCAT (PROMIS program). A.Z.J and I.A.P. also acknowledge the financial support provided by the Serbian Ministry of Education, Science, and Technological Development (Contract number: 451-03-47/2023-01/200146).

Data Availability Statement: There are no additional data to be shared.

Conflicts of Interest: The authors declare no conflict of interest.

References

1. Mikołajczyk, T. The impact of pollutants on catalyst performance during hydrogen evolution reaction: A brief review. *Synth. Met.* **2023**, *296*, 117379. [CrossRef]
2. Angeles-Olvera, Z.; Crespo-Yapur, A.; Rodríguez, O.; Cholula-Díaz, J.L.; Martínez, L.M.; Videa, M. Nickel-Based Electrocatalysts for Water Electrolysis. *Energies* **2022**, *15*, 1609. [CrossRef]
3. Khan, M.A.; Al-Attas, T.; Roy, S.; Rahman, M.M.; Ghaffour, N.; Thangadurai, V.; Larter, S.; Hu, J.; Ajayan, P.M.; Kibria, G. Seawater electrolysis for hydrogen production: A solution looking for a problem? *Energy Environ. Sci.* **2021**, *14*, 4831–4839. [CrossRef]
4. Li, X.; Zhao, L.; Yu, J.; Liu, X.; Zhang, X.; Liu, H.; Zhou, W. Water Splitting: From Electrode to Green Energy System. *Nano-Micro Lett.* **2020**, *12*, 131. [CrossRef] [PubMed]
5. Buriak, J.M.; Toro, C.; Choi, K.-S. Chemistry of Materials for Water Splitting Reactions. *Chem. Mater.* **2018**, *30*, 7325–7327. [CrossRef]

6. Zeng, K.; Zhang, D. Recent progress in alkaline water electrolysis for hydrogen production and applications. *Prog. Energy Combust. Sci.* **2010**, *36*, 307–326. [CrossRef]
7. Yan, Z.; Hitt, J.L.; Turner, J.A.; Mallouk, T.E. Renewable electricity storage using electrolysis. *Proc. Natl. Acad. Sci. USA* **2019**, *117*, 12558–12563. [CrossRef]
8. Zhou, H.; Yu, F.; Zhu, Q.; Sun, J.; Qin, F.; Yu, L.; Bao, J.; Yu, Y.; Chen, S.; Ren, Z. Water splitting by electrolysis at high current densities under 1.6 volts. *Energy Environ. Sci.* **2018**, *11*, 2858–2864. [CrossRef]
9. Guan, D.; Xu, H.; Zhang, Q.; Huang, Y.; Shi, C.; Chang, Y.; Xu, X.; Tang, J.; Gu, Y.; Pao, C.; et al. Identifying A Universal Activity Descriptor and a Unifying Mechanism Concept on Perovskite Oxides for Green Hydrogen Production. *Adv. Mater.* **2023**, e2305074. [CrossRef]
10. International Energy Agency. Net Zero by 2050—A Roadmap for the Global Energy Sector. 2021. Available online: www.iea.org/t&c/ (accessed on 1 September 2023).
11. Guan, D.; Wang, B.; Zhang, J.; Shi, R.; Jiao, K.; Li, L.; Wang, Y.; Xie, B.; Zhang, Q.; Yu, J.; et al. Hydrogen society: From present to future. *Energy Environ. Sci.* **2023**. [CrossRef]
12. Juodkazytė, J.; Seniutinas, G.; Šebeka, B.; Savickaja, I.; Malinauskas, T.; Badokas, K.; Juodkazis, K.; Juodkazis, S. Solar water splitting: Efficiency discussion. *Int. J. Hydrogen Energy* **2016**, *41*, 11941–11948. [CrossRef]
13. Cossar, E.; Murphy, F.; Baranova, E.A. Nickel-based anodes in anion exchange membrane water electrolysis: A review. *J. Chem. Technol. Biotechnol.* **2022**, *97*, 1611–1624. [CrossRef]
14. Raveendran, A.; Chandran, M.; Dhanusuraman, R. A comprehensive review on the electrochemical parameters and recent material development of electrochemical water splitting electrocatalysts. *RSC Adv.* **2023**, *13*, 3843–3876. [CrossRef] [PubMed]
15. Chen, K.; Xu, B.; Shen, L.; Shen, D.; Li, M.; Guo, L.-H. Functions and performance of ionic liquids in enhancing electrocatalytic hydrogen evolution reactions: A comprehensive review. *RSC Adv.* **2022**, *12*, 19452–19469. [CrossRef] [PubMed]
16. Juodkazis, K.; Juodkazytė, J.; Vilkauskaitė, R.; Jasulaitienė, V. Nickel surface anodic oxidation and electrocatalysis of oxygen evolution. *J. Solid State Electrochem.* **2008**, *12*, 1469–1479. [CrossRef]
17. Trasatti, S. Work function, electronegativity, and electrochemical behaviour of metals. *J. Electroanal. Chem. Interfacial Electrochem.* **1972**, *39*, 163–184. [CrossRef]
18. Nørskov, J.K.; Bligaard, T.; Logadottir, A.; Kitchin, J.R.; Chen, J.G.; Pandelov, S.; Stimming, U. Trends in the Exchange Current for Hydrogen Evolution. *J. Electrochem. Soc.* **2005**, *152*, J23. [CrossRef]
19. Sheng, W.; Myint, M.; Chen, J.G.; Yan, Y. Correlating the hydrogen evolution reaction activity in alkaline electrolytes with the hydrogen binding energy on monometallic surfaces. *Energy Environ. Sci.* **2013**, *6*, 1509–1512. [CrossRef]
20. Gutić, S.J.; Dobrota, A.S.; Fako, E.; Skorodumova, N.V.; López, N.; Pašti, I.A. Hydrogen evolution reaction-from single crystal to single atom catalysts. *Catalysts* **2020**, *10*, 290. [CrossRef]
21. Oshchepkov, A. Investigation of the Hydrogen Electrode Reactions on Ni Electrocatalysts in Alkaline Medium. 2017. Available online: https://tel.archives-ouvertes.fr/tel-02003369 (accessed on 1 September 2023).
22. Juodkazis, K.; Juodkazytė, J.; Šebeka, B.; Juodkazis, S. Reversible hydrogen evolution and oxidation on Pt electrode mediated by molecular ion. *Appl. Surf. Sci.* **2014**, *290*, 13–17. [CrossRef]
23. Juodkazis, K.; Juodkazytė, J.; Grigucevičienė, A.; Juodkazis, S. Hydrogen species within the metals: Role of molecular hydrogen ion H_2^+. *Appl. Surf. Sci.* **2011**, *258*, 743–747. [CrossRef]
24. Juodkazytė, J.; Juodkazis, K.; Juodkazis, S. Atoms vs. Ions: Intermediates in reversible electrochemical hydrogen evolution reaction. *Catalysts* **2021**, *11*, 1135. [CrossRef]
25. Kriek, R.J.; Mogwase, B.M.; Vorster, S.W. Relation of the electrochemical interplay between H_2PtCl_6 and $H_2O/H_3O^+/H_2^+$ and the hydrogen-evolution reaction. *Electrochem. Sci. Adv.* **2021**, *2*, e2100041. [CrossRef]
26. Brauns, J.; Turek, T. Alkaline water electrolysis powered by renewable energy: A review. *Processes* **2020**, *8*, 248. [CrossRef]
27. Li, Q.; Villarino, A.M.; Peltier, C.R.; Macbeth, A.J.; Yang, Y.; Kim, M.-J.; Shi, Z.; Krumov, M.R.; Lei, C.; Rodríguez-Calero, G.G.; et al. Anion Exchange Membrane Water Electrolysis: The Future of Green Hydrogen. *J. Phys. Chem. C* **2023**, *127*, 7901–7912. [CrossRef]
28. Murthy, A.P.; Theerthagiri, J.; Madhavan, J. Insights on Tafel Constant in the Analysis of Hydrogen Evolution Reaction. *J. Phys. Chem. C* **2018**, *122*, 23943–23949. [CrossRef]
29. Štrbac, S.; Smiljanić, M.; Wakelin, T.; Potočnik, J.; Rakočević, Z. Hydrogen evolution reaction on bimetallic Ir/Pt(poly) electrodes in alkaline solution. *Electrochim. Acta* **2019**, *306*, 18–27. [CrossRef]
30. Durst, J.; Simon, C.; Siebel, A.; Jan Rheinländer, P.; Schuler, T.; Hanzlik, M.; Herranz, J.; Hasché, F.; Gasteiger, H.A. (Invited) Hydrogen Oxidation and Evolution Reaction (HOR/HER) on Pt Electrodes in Acid vs. Alkaline Electrolytes: Mechanism, Activity and Particle Size Effects. *ECS Trans.* **2014**, *64*, 1069–1080. [CrossRef]
31. Liu, L.; Liu, Y.; Liu, C. Enhancing the Understanding of Hydrogen Evolution and Oxidation Reactions on Pt(111) through Ab Initio Simulation of Electrode/Electrolyte Kinetics. *J. Am. Chem. Soc.* **2020**, *142*, 4985–4989. [CrossRef]
32. Intikhab, S.; Snyder, J.D.; Tang, M.H. Adsorbed Hydroxide Does Not Participate in the Volmer Step of Alkaline Hydrogen Electrocatalysis. *ACS Catal.* **2017**, *7*, 8314–8319. [CrossRef]
33. McCrum, I.T.; Koper, M.T.M. The role of adsorbed hydroxide in hydrogen evolution reaction kinetics on modified platinum. *Nat. Energy* **2020**, *5*, 891–899. [CrossRef]

34. Rheinländer, P.J.; Herranz, J.; Durst, J.; Gasteiger, H.A. Kinetics of the Hydrogen Oxidation/Evolution Reaction on Polycrystalline Platinum in Alkaline Electrolyte Reaction Order with Respect to Hydrogen Pressure. *J. Electrochem. Soc.* **2014**, *161*, F1448–F1457. [CrossRef]
35. Lamoureux, P.S.; Singh, A.R.; Chan, K. pH Effects on Hydrogen Evolution and Oxidation over Pt(111): Insights from First-Principles. *ACS Catal.* **2019**, *9*, 6194–6201. [CrossRef]
36. Shinagawa, T.; Garcia-Esparza, A.T.; Takanabe, K. Insight on Tafel slopes from a microkinetic analysis of aqueous electrocatalysis for energy conversion. *Sci. Rep.* **2015**, *5*, 13801. [CrossRef]
37. Murthy, A.P.; Madhavan, J.; Murugan, K. Recent advances in hydrogen evolution reaction catalysts on carbon/carbon-based supports in acid media. *J. Power Sources* **2018**, *398*, 9–26. [CrossRef]
38. Watzele, S.; Fichtner, J.; Garlyyev, B.; Schwämmlein, J.N.; Bandarenka, A.S. On the Dominating Mechanism of the Hydrogen Evolution Reaction at Polycrystalline Pt Electrodes in Acidic Media. *ACS Catal.* **2018**, *8*, 9456–9462. [CrossRef]
39. Marković, N.M.; Grgur, B.N.; Ross, P.N. Temperature-Dependent Hydrogen Electrochemistry on Platinum Low-Index Single-Crystal Surfaces in Acid Solutions. *J. Phys. Chem. B* **1997**, *101*, 5405–5413. [CrossRef]
40. Greeley, J.; Jaramillo, T.F.; Bonde, J.; Chorkendorff, I.; Nørskov, J.K. Computational high-throughput screening of electrocatalytic materials for hydrogen evolution. *Nat. Mater.* **2006**, *5*, 909–913. [CrossRef]
41. Durst, J.; Simon, C.; Hasché, F.; Gasteiger, H.A. Hydrogen Oxidation and Evolution Reaction Kinetics on Carbon Supported Pt, Ir, Rh, and Pd Electrocatalysts in Acidic Media. *J. Electrochem. Soc.* **2015**, *162*, F190–F203. [CrossRef]
42. Sheng, W.; Gasteiger, H.A.; Shao-Horn, Y. Hydrogen Oxidation and Evolution Reaction Kinetics on Platinum: Acid vs Alkaline Electrolytes. *J. Electrochem. Soc.* **2010**, *157*, B1529. [CrossRef]
43. Durst, J.; Siebel, A.; Simon, C.; Hasché, F.; Herranz, J.; Gasteiger, H.A. New insights into the electrochemical hydrogen oxidation and evolution reaction mechanism. *Energy Environ. Sci.* **2014**, *7*, 2255–2260. [CrossRef]
44. Markovića, N.M.; Sarraf, S.T.; Gasteiger, H.A.; Ross, P.N. Hydrogen electrochemistry on platinum low-index single-crystal surfaces in alkaline solution. *J. Chem. Soc. Faraday Trans.* **1996**, *92*, 3719–3725. [CrossRef]
45. Schmidt, T.; Ross, P.; Markovic, N. Temperature dependent surface electrochemistry on Pt single crystals in alkaline electrolytes: Part 2. The hydrogen evolution/oxidation reaction. *J. Electroanal. Chem.* **2002**, *524–525*, 252–260. [CrossRef]
46. Subbaraman, R.; Tripkovic, D.; Strmcnik, D.; Chang, K.-C.; Uchimura, M.; Paulikas, A.P.; Stamenkovic, V.; Markovic, N.M. Enhancing hydrogen evolution activity in water splitting by tailoring Li^+-$Ni(OH)_2$-Pt interfaces. *Science* **2011**, *334*, 1256–1260. [CrossRef]
47. Subbaraman, R.; Tripkovic, D.; Chang, K.-C.; Strmcnik, D.; Paulikas, A.P.; Hirunsit, P.; Chan, M.; Greeley, J.; Stamenkovic, V. Trends in activity for the water electrolyser reactions on 3d M(Ni,Co,Fe,Mn) hydr(oxy)oxide catalysts. *Nat. Mater.* **2012**, *11*, 550–557. [CrossRef]
48. Katsounaros, I.; Meier, J.C.; Klemm, S.O.; Topalov, A.A.; Biedermann, P.U.; Auinger, M.; Mayrhofer, K.J. The effective surface pH during reactions at the solid–liquid interface. *Electrochem. Commun.* **2011**, *13*, 634–637. [CrossRef]
49. Auinger, M.; Katsounaros, I.; Meier, J.C.; Klemm, S.O.; Biedermann, P.U.; Topalov, A.A.; Rohwerder, M.; Mayrhofer, K.J.J. Near-surface ion distribution and buffer effects during electrochemical reactions. *Phys. Chem. Chem. Phys.* **2011**, *13*, 16384–16394. [CrossRef]
50. Strmcnik, D.; Uchimura, M.; Wang, C.; Subbaraman, R.; Danilovic, N.; van der Vliet, D.; Paulikas, A.P.; Stamenkovic, V.R.; Markovic, N.M. Improving the hydrogen oxidation reaction rate by promotion of hydroxyl adsorption. *Nat. Chem.* **2013**, *5*, 300–306. [CrossRef]
51. Shinagawa, T.; Garcia-Esparza, A.T.; Takanabe, K. Mechanistic Switching by Hydronium Ion Activity for Hydrogen Evolution and Oxidation over Polycrystalline Platinum Disk and Platinum/Carbon Electrodes. *ChemElectroChem* **2014**, *1*, 1497–1507. [CrossRef]
52. Shinagawa, T.; Takanabe, K. Identification of intrinsic catalytic activity for electrochemical reduction of water molecules to generate hydrogen. *Phys. Chem. Chem. Phys.* **2015**, *17*, 15111–15114. [CrossRef]
53. Fuentes-Aceituno, J.; Lapidus, G. A kinetic-mechanistic study of the hydrogen evolution reaction in sulfuric acid solutions with different electrode materials. *J. New Mater. Electrochem. Syst.* **2012**, *15*, 225–231. [CrossRef]
54. Akbayrak, M.; Önal, A.M. High Durability and Electrocatalytic Activity Toward Hydrogen Evolution Reaction with Ultralow Rhodium Loading on Titania. *J. Electrochem. Soc.* **2020**, *167*, 156501. [CrossRef]
55. Gebremariam, G.K.; Jovanović, A.Z.; Dobrota, A.S.; Skorodumova, N.V.; Pašti, I.A. Hydrogen Evolution Volcano(es)—From Acidic to Neutral and Alkaline Solutions. *Catalysts* **2022**, *12*, 1541. [CrossRef]
56. Hall, D.M.; Beck, J.R.; Lvov, S.N. Electrochemical kinetics of the hydrogen reaction on platinum in concentrated HCl(aq). *Electrochem. Commun.* **2015**, *57*, 74–77. [CrossRef]
57. Tang, Z.-Q.; Liao, L.-W.; Zheng, Y.-L.; Kang, J.; Chen, Y.-X. Temperature Effect on Hydrogen Evolution Reaction at Au Electrode. *Chin. J. Chem. Phys.* **2012**, *25*, 469. [CrossRef]
58. Zheng, Y.; Jiao, Y.; Vasileff, A.; Qiao, S.-Z. The Hydrogen Evolution Reaction in Alkaline Solution: From Theory, Single Crystal Models, to Practical Electrocatalysts. *Angew. Chem. Int. Ed.* **2018**, *57*, 7568–7579. [CrossRef]
59. Badawy, W.; Feky, H.; Helal, N.; Mohammed, H. Cathodic hydrogen evolution on molybdenum in NaOH solutions. *Int. J. Hydrogen Energy* **2013**, *38*, 9625–9632. [CrossRef]
60. Meethal, R.P.; Saibi, R.; Srinivasan, R. Hydrogen evolution reaction on polycrystalline Au inverted rotating disc electrode in HClO4 and NaOH solutions. *Int. J. Hydrogen Energy* **2022**, *47*, 14304–14318. [CrossRef]

61. Chanda, D.; Hnát, J.; Dobrota, A.S.; Pašti, I.A.; Paidar, M.; Bouzek, K. The effect of surface modification by reduced graphene oxide on the electrocatalytic activity of nickel towards the hydrogen evolution reaction. *Phys. Chem. Chem. Phys.* **2015**, *17*, 26864–26874. [CrossRef]
62. Bao, F.; Kemppainen, E.; Dorbandt, I.; Bors, R.; Xi, F.; Schlatmann, R.; van de Krol, R.; Calnan, S. Understanding the Hydrogen Evolution Reaction Kinetics of Electrodeposited Nickel-Molybdenum in Acidic, Near-Neutral, and Alkaline Conditions. *ChemElectroChem* **2020**, *8*, 195–208. [CrossRef]
63. Petrii, O.A.; Tsirlina, G.A. Electrocatalytic activity prediction for hydrogen electrode reaction: Intuition, art, science. *Electrochimica Acta* **1994**, *39*, 1739–1747. [CrossRef]
64. Miousse, D.; Lasia, A.; Borck, V. Hydrogen evolution reaction on Ni-Al-Mo and Ni-Al electrodes prepared by low pressure plasma spraying. *J. Appl. Electrochem.* **1995**, *25*, 592–602. [CrossRef]
65. Tang, D.; Lu, J.; Zhuang, L.; Liu, P. Calculations of the exchange current density for hydrogen electrode reactions: A short review and a new equation. *J. Electroanal. Chem.* **2010**, *644*, 144–149. [CrossRef]
66. Ernst, S.; Hamann, C. The pH-dependence of the hydrogen exchange current density at smooth platinum in alkaline solution (KOH). *J. Electroanal. Chem. Interfacial Electrochem.* **1975**, *60*, 97–100. [CrossRef]
67. Santos, D.; Sequeira, C.; Macciò, D.; Saccone, A.; Figueiredo, J. Platinum–rare earth electrodes for hydrogen evolution in alkaline water electrolysis. *Int. J. Hydrogen Energy* **2013**, *38*, 3137–3145. [CrossRef]
68. Amaral, L.; Cardoso, D.; Šljukić, B.; Santos, D.; Sequeira, C. Electrochemistry of hydrogen evolution in ionic liquids aqueous mixtures. *Mater. Res. Bull.* **2019**, *112*, 407–412. [CrossRef]
69. Zhou, Z.; Pei, Z.; Wei, L.; Zhao, S.; Jian, X.; Chen, Y. Electrocatalytic hydrogen evolution under neutral pH conditions: Current understandings, recent advances, and future prospects. *Energy Environ. Sci.* **2020**, *13*, 3185–3206. [CrossRef]
70. Xie, X.; Song, M.; Wang, L.; Engelhard, M.H.; Luo, L.; Miller, A.; Zhang, Y.; Du, L.; Pan, H.; Nie, Z.; et al. Electrocatalytic Hydrogen Evolution in Neutral pH Solutions: Dual-Phase Synergy. *ACS Catal.* **2019**, *9*, 8712–8718. [CrossRef]
71. Merrill, M.D.; Logan, B.E. Electrolyte effects on hydrogen evolution and solution resistance in microbial electrolysis cells. *J. Power Sources* **2009**, *191*, 203–208. [CrossRef]
72. Weber, D.J.; Janssen, M.; Oezaslan, M. Effect of Monovalent Cations on the HOR/HER Activity for Pt in Alkaline Environment. *J. Electrochem. Soc.* **2019**, *166*, F66–F73. [CrossRef]
73. Guha, A.; Kaley, N.M.; Mondal, J.; Narayanan, T.N. Engineering the hydrogen evolution reaction of transition metals: Effect of Li ions. *J. Mater. Chem. A* **2020**, *8*, 15795–15808. [CrossRef]
74. Conway, B.; Tilak, B. Interfacial processes involving electrocatalytic evolution and oxidation of H_2, and the role of chemisorbed H. *Electrochim. Acta* **2002**, *47*, 3571–3594. [CrossRef]
75. Sheng, W. Correlating hydrogen oxidation and evolution activity on platinum at different pH with measured hydrogen binding energy. *Nat. Commun.* **2015**, *6*, 5848. [CrossRef] [PubMed]
76. McCrum, I.T.; Janik, M.J. pH and Alkali Cation Effects on the Pt Cyclic Voltammogram Explained Using Density Functional Theory. *J. Phys. Chem. C* **2015**, *120*, 457–471. [CrossRef]
77. Kim, H.; Hong, J.; Park, K.-Y.; Kim, H.; Kim, S.-W.; Kang, K. Aqueous rechargeable Li and Na ion batteries. *Chem. Rev.* **2014**, *114*, 11788–11827. [CrossRef]
78. Suo, L.; Borodin, O.; Gao, T.; Olguin, M.; Ho, J.; Fan, X.; Luo, C.; Wang, C.; Xu, K. "Water-in-salt" electrolyte enables high-voltage aqueous lithium-ion chemistries. *Science* **2015**, *350*, 938–943. [CrossRef]
79. Laursen, A.B.; Varela, A.S.; Dionigi, F.; Fanchiu, H.; Miller, C.; Trinhammer, O.L.; Rossmeisl, J.; Dahl, S. Electrochemical hydrogen evolution: Sabatiers principle and the volcano plot. *J. Chem. Educ.* **2012**, *89*, 1595–1599. [CrossRef]
80. Herranz, J.; Durst, J.; Fabbri, E.; Pătru, A.; Cheng, X.; Permyakova, A.A.; Schmidt, T.J. Interfacial effects on the catalysis of the hydrogen evolution, oxygen evolution and CO_2-reduction reactions for (co-)electrolyzer development. *Nano Energy* **2016**, *29*, 4–28. [CrossRef]
81. Strmcnik, D.; Lopes, P.P.; Genorio, B.; Stamenkovic, V.R.; Markovic, N.M. Design principles for hydrogen evolution reaction catalyst materials. *Nano Energy* **2016**, *29*, 29–36. [CrossRef]
82. Marković, N.; Ross, P.N., Jr. Surface science studies of model fuel cell electrocatalysts. *Surf. Sci. Rep.* **2002**, *45*, 117–229. [CrossRef]
83. Danilovic, N.; Subbaraman, R.; Strmcnik, D.; Stamenkovic, V.; Markovic, N. Electrocatalysis of the HER in acid and alkaline media. *J. Serbian Chem. Soc.* **2013**, *78*, 2007–2015. [CrossRef]
84. Zheng, J.; Sheng, W.; Zhuang, Z.; Xu, B.; Yan, Y. Universal dependence of hydrogen oxidation and evolution reaction activity of platinum-group metals on pH and hydrogen binding energy. *Sci. Adv.* **2016**, *2*, e1501602. [CrossRef] [PubMed]
85. Wang, Y.; Wang, G.; Li, G.; Huang, B.; Pan, J.; Liu, Q.; Han, J.; Xiao, L.; Lu, J.; Zhuang, L. Pt–Ru catalyzed hydrogen oxidation in alkaline media: Oxophilic effect or electronic effect? *Energy Environ. Sci.* **2014**, *8*, 177–181. [CrossRef]
86. van der Niet, M.J.; Garcia-Araez, N.; Hernández, J.; Feliu, J.M.; Koper, M.T. Water dissociation on well-defined platinum surfaces: The electrochemical perspective. *Catal. Today* **2013**, *202*, 105–113. [CrossRef]
87. Marković, N.M.; Schmidt, T.J.; Grgur, B.N.; Gasteiger, H.A.; Behm, R.J.; Ross, P.N. Effect of Temperature on Surface Processes at the Pt(111)−Liquid Interface: Hydrogen Adsorption, Oxide Formation, and CO Oxidation. *J. Phys. Chem. B* **1999**, *103*, 8568–8577. [CrossRef]
88. Ledezma-Yanez, I.; Wallace, W.D.Z.; Sebastián-Pascual, P.; Climent, V.; Feliu, J.M.; Koper, M.T.M. Interfacial water reorganization as a pH-dependent descriptor of the hydrogen evolution rate on platinum electrodes. *Nat. Energy* **2017**, *2*, 17031. [CrossRef]

89. Rossmeisl, J.; Chan, K.; Ahmed, R.; Tripković, V.; Björketun, M.E. pH in atomic scale simulations of electrochemical interfaces. *Phys. Chem. Chem. Phys.* **2013**, *15*, 10321–10325. [CrossRef]
90. Rossmeisl, J.; Chan, K.; Skúlason, E.; Björketun, M.E.; Tripkovic, V. On the pH dependence of electrochemical proton transfer barriers. *Catal. Today* **2016**, *262*, 36–40. [CrossRef]
91. Cheng, T.; Wang, L.; Merinov, B.V.; Goddard, W.A. Explanation of Dramatic pH-Dependence of Hydrogen Binding on Noble Metal Electrode: Greatly Weakened Water Adsorption at High pH. *J. Am. Chem. Soc.* **2018**, *140*, 7787–7790. [CrossRef]
92. Shinagawa, T.; Takanabe, K. Electrolyte Engineering toward Efficient Hydrogen Production Electrocatalysis with Oxygen-Crossover Regulation under Densely Buffered Near-Neutral pH Conditions. *J. Phys. Chem. C* **2016**, *120*, 1785–1794. [CrossRef]
93. Murthy, A.P.; Govindarajan, D.; Theerthagiri, J.; Madhavan, J.; Parasuraman, K. Metal-doped molybdenum nitride films for enhanced hydrogen evolution in near-neutral strongly buffered aerobic media. *Electrochim. Acta* **2018**, *283*, 1525–1533. [CrossRef]
94. Shinagawa, T.; Takanabe, K. Electrocatalytic Hydrogen Evolution under Densely Buffered Neutral pH Conditions. *J. Phys. Chem. C* **2015**, *119*, 20453–20458. [CrossRef]
95. Shinagawa, T.; Takanabe, K. Towards Versatile and Sustainable Hydrogen Production through Electrocatalytic Water Splitting: Electrolyte Engineering. *ChemSusChem* **2017**, *10*, 1318–1336. [CrossRef] [PubMed]
96. Kanan, M.W.; Nocera, D.G. In situ formation of an oxygen-evolving catalyst in neutral water containing phosphate and Co^{2+}. *Science* **2008**, *321*, 1072–1075. [CrossRef] [PubMed]
97. Lutterman, D.A.; Surendranath, Y.; Nocera, D.G. A self-healing oxygen-evolving catalyst. *J. Am. Chem. Soc.* **2009**, *131*, 3838–3839. [CrossRef]
98. Kanan, M.W.; Yano, J.; Surendranath, Y.; Dincă, M.; Yachandra, V.K.; Nocera, D.G. Structure and valency of a cobalt-phosphate water oxidation catalyst determined by in situ X-ray spectroscopy. *J. Am. Chem. Soc.* **2010**, *132*, 13692–13701. [CrossRef]
99. Marcandalli, G.; Boterman, K.; Koper, M.T. Understanding hydrogen evolution reaction in bicarbonate buffer. *J. Catal.* **2021**, *405*, 346–354. [CrossRef]
100. Muñoz, L.D.S.; Bergel, A.; Féron, D.; Basséguy, R. Hydrogen production by electrolysis of a phosphate solution on a stainless steel cathode. *Int. J. Hydrogen Energy* **2010**, *35*, 8561–8568. [CrossRef]
101. Zhu, S.; Qin, X.; Yao, Y.; Shao, M. PH-Dependent Hydrogen and Water Binding Energies on Platinum Surfaces as Directly Probed through Surface-Enhanced Infrared Absorption Spectroscopy. *J. Am. Chem. Soc.* **2020**, *142*, 8748–8754. [CrossRef]
102. Sun, Y.; Liu, C.; Grauer, D.C.; Yano, J.; Long, J.R.; Yang, P.; Chang, C.J. Electrodeposited cobalt-sulfide catalyst for electrochemical and photoelectrochemical hydrogen generation from water. *J. Am. Chem. Soc.* **2013**, *135*, 17699–17702. [CrossRef]
103. Zhang, R.; Pearce, P.E.; Duan, Y.; Dubouis, N.; Marchandier, T.; Grimaud, A. Importance of Water Structure and Catalyst–Electrolyte Interface on the Design of Water Splitting Catalysts. *Chem. Mater.* **2019**, *31*, 8248–8259. [CrossRef]
104. Strmcnik, D.; Kodama, K.; van der Vliet, D.; Greeley, J.; Stamenkovic, V.R.; Marković, N.M. The role of non-covalent interactions in electrocatalytic fuel-cell reactions on platinum. *Nat. Chem.* **2009**, *1*, 466–472. [CrossRef] [PubMed]
105. Tymoczko, J.; Colic, V.; Ganassin, A.; Schuhmann, W.; Bandarenka, A.S. Influence of the alkali metal cations on the activity of Pt(111) towards model electrocatalytic reactions in acidic sulfuric media. *Catal. Today* **2015**, *244*, 96–102. [CrossRef]
106. Strmcnik, D.; van der Vliet, D.F.; Chang, K.-C.; Komanicky, V.; Kodama, K.; You, H.; Stamenkovic, V.R.; Marković, N.M. Effects of Li^+, K^+, and Ba^{2+} cations on the ORR at model and high surface area Pt and Au surfaces in alkaline solutions. *J. Phys. Chem. Lett.* **2011**, *2*, 2733–2736. [CrossRef]
107. García, N.; Climent, V.; Orts, J.M.; Feliu, J.M.; Aldaz, A. Effect of pH and alkaline metal cations on the voltammetry of Pt(111) single crystal electrodes in sulfuric acid solution. *ChemPhysChem* **2004**, *5*, 1221–1227. [CrossRef] [PubMed]
108. Liu, E.; Li, J.; Jiao, L.; Doan, H.T.T.; Liu, Z.; Zhao, Z.; Huang, Y.; Abraham, K.M.; Mukerjee, S.; Jia, Q. Unifying the Hydrogen Evolution and Oxidation Reactions Kinetics in Base by Identifying the Catalytic Roles of Hydroxyl-Water-Cation Adducts. *J. Am. Chem. Soc.* **2019**, *141*, 3232–3239. [CrossRef]
109. Xue, S.; Garlyyev, B.; Watzele, S.; Liang, Y.; Fichtner, J.; Pohl, M.D.; Bandarenka, A.S. Influence of Alkali Metal Cations on the Hydrogen Evolution Reaction Activity of Pt, Ir, Au, and Ag Electrodes in Alkaline Electrolytes. *ChemElectroChem* **2018**, *5*, 2326–2329. [CrossRef]
110. Dubouis, N.; Grimaud, A. The hydrogen evolution reaction: From material to interfacial descriptors. *Chem. Sci.* **2019**, *10*, 9165–9181. [CrossRef]
111. Huang, B.; Rao, R.R.; You, S.; Myint, K.H.; Song, Y.; Wang, Y.; Ding, W.; Giordano, L.; Zhang, Y.; Wang, T.; et al. Cation- and pH-Dependent Hydrogen Evolution and Oxidation Reaction Kinetics. *JACS Au* **2021**, *1*, 1674–1687. [CrossRef]
112. Monteiro, M.C.O.; Goyal, A.; Moerland, P.; Koper, M.T.M. Understanding Cation Trends for Hydrogen Evolution on Platinum and Gold Electrodes in Alkaline Media. *ACS Catal.* **2021**, *11*, 14328–14335. [CrossRef]
113. Guha, A.; Narayanan, T.N. Effect of 'water-in-salt' electrolytes in the electrochemical hydrogen evolution reaction of carbon nanotubes. *J. Phys. Energy* **2020**, *2*, 034001. [CrossRef]
114. Guha, A.; Narayanaru, S.; Narayanan, T.N. Tuning the Hydrogen Evolution Reaction on Metals by Lithium Salt. *ACS Appl. Energy Mater.* **2018**, *1*, 7116–7122. [CrossRef]
115. Monteiro, M.C.O.; Dattila, F.; Hagedoorn, B.; García-Muelas, R.; López, N.; Koper, M.T.M. Absence of CO_2 electroreduction on copper, gold and silver electrodes without metal cations in solution. *Nat. Catal.* **2021**, *4*, 654–662. [CrossRef]
116. Marcandalli, G.; Goyal, A.; Koper, M.T.M. Electrolyte Effects on the Faradaic Efficiency of CO_2 Reduction to CO on a Gold Electrode. *ACS Catal.* **2021**, *11*, 4936–4945. [CrossRef] [PubMed]

117. Marcandalli, G.; Monteiro, M.C.O.; Goyal, A.; Koper, M.T.M. Electrolyte Effects on CO_2 Electrochemical Reduction to CO. *Accounts Chem. Res.* **2022**, *55*, 1900–1911. [CrossRef]
118. Ye, C.; Dattila, F.; Chen, X.; López, N.; Koper, M.T.M. Influence of Cations on HCOOH and CO Formation during CO_2 Reduction on a $Pd_{ML}Pt(111)$ Electrode. *J. Am. Chem. Soc.* **2023**, *145*, 19601–19610. [CrossRef]
119. Matanovic, I.; Atanassov, P.; Garzon, F.; Henson, N.J. Density Functional Theory Study of the Alkali Metal Cation Adsorption on Pt(111), Pt(100), and Pt(110) Surfaces. *ECS Trans.* **2014**, *61*, 47–53. [CrossRef]
120. Garlyyev, B.; Xue, S.; Watzele, S.; Scieszka, D.; Bandarenka, A.S. Influence of the Nature of the Alkali Metal Cations on the Electrical Double-Layer Capacitance of Model Pt(111) and Au(111) Electrodes. *J. Phys. Chem. Lett.* **2018**, *9*, 1927–1930. [CrossRef]
121. Mills, J.N.; McCrum, I.T.; Janik, M.J. Alkali cation specific adsorption onto fcc(111) transition metal electrodes. *Phys. Chem. Chem. Phys.* **2014**, *16*, 13699–13707. [CrossRef]
122. Taji, Y.; Zagalskaya, A.; Evazzade, I.; Watzele, S.; Song, K.-T.; Xue, S.; Schott, C.; Garlyyev, B.; Alexandrov, V.; Gubanova, E.; et al. Alkali metal cations change the hydrogen evolution reaction mechanisms at Pt electrodes in alkaline media. *Nano Mater. Sci.* **2022**. [CrossRef]
123. Goyal, A.; Koper, M.T.M. The Interrelated Effect of Cations and Electrolyte pH on the Hydrogen Evolution Reaction on Gold Electrodes in Alkaline Media. *Angew. Chem. Int. Ed.* **2021**, *60*, 13452–13462. [CrossRef] [PubMed]
124. Kamat, G.A.; Zeledón, J.A.Z.; Gunasooriya, G.T.K.K.; Dull, S.M.; Perryman, J.T.; Nørskov, J.K.; Stevens, M.B.; Jaramillo, T.F. Acid anion electrolyte effects on platinum for oxygen and hydrogen electrocatalysis. *Commun. Chem.* **2022**, *5*, 20. [CrossRef] [PubMed]
125. Lamy-Pitara, E.; El Mouahid, S.; Barbier, J. Effect of anions on catalytic and electrocatalytic hydrogenations and on the electrocatalytic oxidation and evolution of hydrogen on platinum. *Electrochimica Acta* **2000**, *45*, 4299–4308. [CrossRef]
126. Quaino, P.; Juarez, F.; Santos, E.; Schmickler, W. Volcano plots in hydrogen electrocatalysis—Uses and abuses. *Beilstein J. Nanotechnol.* **2014**, *5*, 846–854. [CrossRef]
127. Komiya, H.; Obata, K.; Wada, M.; Nishimoto, T.; Takanabe, K. Electrolyte Engineering Applying Concentrated Chloride Ions with Mixed Buffer Solutions for a Versatile High-Productivity Water-Splitting System. *ACS Sustain. Chem. Eng.* **2023**, *11*, 12614–12622. [CrossRef]
128. Arminio-Ravelo, J.A.; Jensen, A.W.; Jensen, K.D.; Quinson, J.; Escudero-Escribano, M. Electrolyte Effects on the Electrocatalytic Performance of Iridium-Based Nanoparticles for Oxygen Evolution in Rotating Disc Electrodes. *Chemphyschem* **2019**, *20*, 2956–2963. [CrossRef]
129. Faid, A.Y.; Foroughi, F.; Sunde, S.; Pollet, B. Unveiling hydrogen evolution dependence on KOH concentration for polycrystalline and nanostructured nickel-based catalysts. *J. Appl. Electrochem.* **2022**, *52*, 1819–1826. [CrossRef]
130. Li, D.; Park, E.J.; Zhu, W.; Shi, Q.; Zhou, Y.; Tian, H.; Lin, Y.; Serov, A.; Zulevi, B.; Baca, E.D.; et al. Highly quaternized polystyrene ionomers for high performance anion exchange membrane water electrolysers. *Nat. Energy* **2020**, *5*, 378–385. [CrossRef]
131. Kuznetsov, A.N.; Oshchepkov, A.G.; Cherstiouk, O.V.; Simonov, P.A.; Nazmutdinov, R.R.; Savinova, E.R.; Bonnefont, A. Influence of the NaOH Concentration on the Hydrogen Electrode Reaction Kinetics of Ni and NiCu Electrodes. *ChemElectroChem* **2020**, *7*, 1438–1447. [CrossRef]
132. Cossar, E.; Houache, M.S.; Zhang, Z.; Baranova, E.A. Comparison of electrochemical active surface area methods for various nickel nanostructures. *J. Electroanal. Chem.* **2020**, *870*, 114246. [CrossRef]
133. Shinagawa, T.; Takanabe, K. Impact of solute concentration on the electrocatalytic conversion of dissolved gases in buffered solutions. *J. Power Sources* **2015**, *287*, 465–471. [CrossRef]
134. Barwe, S.; Mei, B.; Masa, J.; Schuhmann, W.; Ventosa, E. Overcoming cathode poisoning from electrolyte impurities in alkaline electrolysis by means of self-healing electrocatalyst films. *Nano Energy* **2018**, *53*, 763–768. [CrossRef]
135. Weber, D.J.; Dosche, C.; Oezaslan, M. Fundamental Aspects of Contamination during the Hydrogen Evolution/Oxidation Reaction in Alkaline Media. *J. Electrochem. Soc.* **2020**, *167*, 024506. [CrossRef]
136. Li, X.; Gunathunge, C.M.; Agrawal, N.; Montalvo-Castro, H.; Jin, J.; Janik, M.J.; Waegele, M.M. Impact of Alkali Metal Cations and Iron Impurities on the Evolution of Hydrogen on Cu Electrodes in Alkaline Electrolytes. *J. Electrochem. Soc.* **2020**, *167*, 106505. [CrossRef]
137. Klaus, S.; Cai, Y.; Louie, M.W.; Trotochaud, L.; Bell, A.T. Effects of Fe electrolyte impurities on $Ni(OH)_2/NiOOH$ structure and oxygen evolution activity. *J. Phys. Chem. C* **2015**, *119*, 7243–7254. [CrossRef]
138. Salmanion, M.; Najafpour, M.M. Oxygen-evolution reaction by gold and cobalt in iron and nickel free electrolyte. *Int. J. Hydrogen Energy* **2020**, *46*, 1509–1516. [CrossRef]
139. Klaus, S.; Trotochaud, L.; Cheng, M.-J.; Head-Gordon, M.; Bell, A.T. Experimental and Computational Evidence of Highly Active Fe Impurity Sites on the Surface of Oxidized Au for the Electrocatalytic Oxidation of Water in Basic Media. *ChemElectroChem* **2015**, *3*, 66–73. [CrossRef]
140. Gong, L.; Koh, J.R.; Yeo, B.S. Mechanistic Study of the Synergy between Iron and Transition Metals for the Catalysis of the Oxygen Evolution Reaction. *ChemSusChem* **2018**, *11*, 3790–3795. [CrossRef]
141. Bockris, J.O.; Conway, B.E. Studies in hydrogen overpotential. The effect of catalytic poisons at platinized platinum and nickel. *Trans. Faraday Soc.* **1949**, *45*, 989–999. [CrossRef]
142. Gao, L.; Conway, B. Poisoning effects of arsenic species on H adsorption and kinetic behaviour of the H2 evolution reaction at Pt in KOH solution. *J. Electroanal. Chem.* **1995**, *395*, 261–271. [CrossRef]

143. Gao, L.J.; Qian, S.Y.; Conway, B.E. Arsenic poisoning effects on cathodic polarization and hydrogen adsorption at platinum and steel electrodes in KF · 2HF melts. *J. Appl. Electrochem.* **1996**, *26*, 803–814. [CrossRef]
144. Becker, H.; Murawski, J.; Shinde, D.V.; Stephens, I.E.L.; Hinds, G.; Smith, G. Impact of impurities on water electrolysis: A review. *Sustain. Energy Fuels* **2023**, *7*, 1565–1603. [CrossRef]
145. Bhattacharyya, S.; Das, C.; Maji, T.K. MOF derived carbon based nanocomposite materials as efficient electrocatalysts for oxygen reduction and oxygen and hydrogen evolution reactions. *RSC Adv.* **2018**, *8*, 26728–26754. [CrossRef]
146. Pumera, M. Materials Electrochemists' Never-Ending Quest for Efficient Electrocatalysts: The Devil Is in the Impurities. *ACS Catal.* **2020**, *10*, 7087–7092. [CrossRef]
147. Wang, L.; Sofer, Z.; Pumera, M. Will Any Crap We Put into Graphene Increase Its Electrocatalytic Effect? *ACS Nano* **2020**, *14*, 21–25. [CrossRef] [PubMed]
148. Guan, D.; Ryu, G.; Hu, Z.; Zhou, J.; Dong, C.-L.; Huang, Y.-C.; Zhang, K.; Zhong, Y.; Komarek, A.C.; Zhu, M.; et al. Utilizing ion leaching effects for achieving high oxygen-evolving performance on hybrid nanocomposite with self-optimized behaviors. *Nat. Commun.* **2020**, *11*, 3376. [CrossRef]